Cellular/Molecular

Selective Manipulation of G-Protein γ_7 Subunit in Mice Provides New Insights into Striatal Control of Motor Behavior

Gloria Brunori, Oliver B. Pelletier, Anna M. Stauffer, and Janet D. Robishaw
Department of Biomedical Science, Charles E. Schmidt College of Medicine, Florida Atlantic University, Boca Raton, Florida, 33431

Stimulatory coupling of dopamine D_1 (D_1R) and adenosine A_{2A} receptors ($A_{2A}R$) to adenylyl cyclase within the striatum is mediated through a specific $G\alpha_{olf}\beta_2\gamma_7$ heterotrimer to ultimately modulate motor behaviors. To dissect the individual roles of the $G\alpha_{olf}\beta_2\gamma_7$ heterotrimer in different populations of medium spiny neurons (MSNs), we produced and characterized conditional mouse models, in which the *Gng7* gene was deleted in either the D_1R- or $A_{2A}R/D_2R$-expressing MSNs. We show that conditional loss of γ_7 disrupts the cell type-specific assembly of the $G\alpha_{olf}\beta_2\gamma_7$ heterotrimer, thereby identifying its circumscribed roles acting downstream of either the D_1Rs or $A_{2A}Rs$ in coordinating motor behaviors, including *in vivo* responses to psychostimulants. We reveal that $G\alpha_{olf}\beta_2\gamma_7$/cAMP signal in D_1R-MSNs does not impact spontaneous and amphetamine-induced locomotor behaviors in male and female mice, while its loss in $A_{2A}R/D_2R$-MSNs results in a hyperlocomotor phenotype and enhanced locomotor response to amphetamine. Additionally, $G\alpha_{olf}\beta_2\gamma_7$/cAMP signal in either D_1R- or $A_{2A}R/D_2R$-expressing MSNs is not required for the activation of PKA signaling by amphetamine. Finally, we show that $G\alpha_{olf}\beta_2\gamma_7$ signaling acting downstream of D_1Rs is selectively implicated in the acute locomotor-enhancing effects of morphine. Collectively, these results support the general notion that receptors use specific $G\alpha\beta\gamma$ proteins to direct the fidelity of downstream signaling pathways and to elicit a diverse repertoire of cellular functions. Specifically, these findings highlight the critical role for the γ_7 protein in determining the cellular level, and hence, the function of the $G\alpha_{olf}\beta_2\gamma_7$ heterotrimer in several disease states associated with dysfunctional striatal signaling.

Key words: **amphetamine; cAMP; dopamine; G-protein; locomotion; striatum**

Significance Statement

Dysfunction or imbalance of cAMP signaling in the striatum has been linked to several neurologic and neuropsychiatric disorders, including Parkinson's disease, dystonia, schizophrenia, and drug addiction. By genetically targeting the γ_7 subunit in distinct striatal neuronal subpopulations in mice, we demonstrate that the formation and function of the $G\alpha_{olf}\beta_2\gamma_7$ heterotrimer, which represents the rate-limiting step for cAMP production in the striatum, is selectively disrupted. Furthermore, we reveal cell type-specific roles for $G\alpha_{olf}\beta_2\gamma_7$-mediated cAMP production in the control of spontaneous locomotion as well as behavioral and molecular responses to psychostimulants. Our findings identify the γ_7 protein as a novel therapeutic target for disease states associated with dysfunctional striatal cAMP signaling.

Introduction

The G-protein coupled receptor (GPCR) superfamily is comprised of several hundred receptors, which are responsible for converting extracellular information into the appropriate cellular responses (Rosenbaum et al., 2009; Roth et al., 2017). Along with the increasing diversity and complexity, there is a growing awareness of the importance of spatial organization of GPCR–effector complexes in regulating their specificity and efficiency (Robishaw and Berlot, 2004; Bychkov et al., 2012; Yano et al., 2018). Perhaps nowhere is this complexity and spatial organization more important than in the striatum (Xie and Martemyanov, 2011; Bychkov et al., 2012; Peterson et al., 2015), wherein multiple neurotransmitters and neuromodulators converge onto different GPCRs to affect cell excitability and shape long-term synaptic plasticity (Lovinger, 2010; Gerfen and Surmeier, 2011). Within the striatum, there are two distinct classes of GABAergic medium spiny neurons (MSNs): the dopamine D_1 receptor (D_1R)-expressing MSNs

Received June 10, 2021; revised Aug. 26, 2021; accepted Sep. 11, 2021.

Author contributions: G.B. and J.D.R. designed research; G.B., O.B.P., and A.M.S. performed research; G.B. analyzed data; G.B. wrote the paper; J.D.R. edited the paper.

This work was supported by National Institutes of Health Grant GM114665 to J.D.R. We thank Dr. Andrea Cippitelli, Dr. Gerda Breitwieser, and Dr. Lawrence Toll for critical comments on the manuscript; Dr. Denis Hervé and Dr. Kirill Martemyanov for providing the $G\alpha_{olf}$ and the AC5 antibodies, respectively; and the Cell Imaging and Neurobehavior Core facilities at the Florida Atlantic University Brain Institute.

The authors declare no competing financial interests.

Correspondence should be addressed to Janet D. Robishaw at jrobishaw@health.fau.edu.

https://doi.org/10.1523/JNEUROSCI.1211-21.2021

and the dopamine D_2 receptor (D_2R)- and adenosine A_{2A} receptor ($A_{2A}R$)-expressing MSNs (Gerfen et al., 1990). By converging via different neurocircuitries on the thalamus (e.g., D_1R-striatonigral and D_2R-striatopallidal pathways), signaling via D_1R-MSNs stimulate spontaneous and acquired motor behaviors, whereas D_2R-MSNs activation inhibits motor activities (Kravitz et al., 2010; Durieux et al., 2012; Farrell et al., 2013). The striatum also contains a small population of cholinergic and GABAergic interneurons, which further tune the activity of both D_1R- and D_2R-MSNs (Tepper et al., 2018; Abudukeyoumu et al., 2019). Given the complex neural circuitry and number of GPCRs within the striatum, a comprehensive understanding of how this multitude of signaling outputs are tailored to various cell types and elicited by diverse stimuli is lacking. One unanswered question revolves around whether receptors bind to specific $G\alpha\beta\gamma$ heterotrimers to mediate particular cellular responses. In this regard, combinatorial association of the known number of distinct G-protein α, β, and γ subtypes has been postulated to provide the level of selectivity that is needed to act downstream of a similarly large number of receptors (Robishaw and Berlot, 2004; Khan et al., 2013; Yim et al., 2020; Masuho et al., 2021).

In this paper, we sought to address this question by targeting the specific G-protein acting downstream of the D_1R and $A_{2A}R$. Initially identified in the sensory neurons of the olfactory epithelium (Jones and Reed, 1989; Belluscio et al., 1998), the stimulatory G-protein α_{olf} is expressed in nearly all MSNs. Previous analyses of mice lacking the *Gnal* gene revealed that $G\alpha_{olf}$ is required for the coupling of D_1R and $A_{2A}R$ to the adenylyl cyclase (AC)/cAMP signaling pathway (Corvol et al., 2001). Because complete loss of $G\alpha_{olf}$ is associated with an olfactory-dependent suckling defect and high perinatal lethality (Belluscio et al., 1998), further studies have been largely restricted to mice carrying a single *Gnal* null mutation ($Gnal^{+/-}$) to probe important functions of $G\alpha_{olf}$-mediated signal in striatal-dependent motor behavior and reward-related processes (Herve et al., 2001; Corvol et al., 2007). More recently, the $G\beta\gamma$ dimers associated with $G\alpha_{olf}$ have been identified. While α_{olf} pairs with the γ_{13} subunit in the olfactory epithelium (Kerr et al., 2008; Li et al., 2013), the majority of α_{olf} subunit (>80%) shows a specific requirement for the γ_7 subunit in the assembly of the $G_{olf}\beta_2\gamma_7$ heterotrimer that is critical for stimulation of AC activity in the striatum (Schwindinger et al., 2003, 2010). This finding offers an effective and selective mean of disrupting the striatal specific $G\alpha_{olf}\beta_2\gamma_7$ heterotrimer without incurring the confounding effects of olfactory dysfunction.

In this study, two new conditional mouse models, in which the *Gng7* gene is deleted specifically in either D_1R- or D_2R/$A_{2A}R$-expressing MSNs, were produced and characterized. Using anatomic, molecular, and biochemical approaches, we extended prior work by showing that γ_7 directs the ordered assembly of $G\alpha_{olf}\beta_2\gamma_7$ heterotrimer acting downstream of the D_1Rs and $A_{2A}Rs$ in two distinct MSN populations. Moreover, using a battery of behavioral phenotyping tests, we identified circumscribed roles for D_1R-$G\alpha_{olf}\beta_2\gamma_7$ and $A_{2A}R$-$G\alpha_{olf}\beta_2\gamma_7$ signaling in striatal-dependent modulation of motor behaviors and *in vivo* responses to psychostimulants.

Materials and Methods

Generation of Gng7 conditional KO mice. Floxed *Gng7* mice ($Gng7^{fl/fl}$), with both alleles of the gene encoding the G-protein γ_7 subunit flanked by loxP sites (Schwindinger et al., 2003), were backcrossed with FLPe recombinase knock-in mice (Jackson ImmunoResearch Laboratories) to excise the FRT flanked neomycin cassette. $D1Cre^+$ (Drd1a; EY262) and $D2Cre^+$ (Drd2; ER44) BAC transgenic mice were purchased from the Mutant Mouse Regional Resource Center (Gong et al., 2007). To generate conditional KO mice used in these studies, $Gng7^{fl/fl}$ were bred to either $D1Cre^+$ or $D2Cre^+$ for two generations to obtain $Gng7^{fl/fl}D1Cre^+$ or $Gng7^{fl/fl}D2Cre^+$ and $Gng7^{fl/fl}$ WT littermates. Mice were maintained by backcrosses to C57BL6/J every 5 or 6 generations (Jackson ImmunoResearch Laboratories). Recombination of the floxed alleles and genotypes was confirmed by PCR of tail biopsies and brain tissues, using primers described previously (Schwindinger et al., 2003). Subsequently, mice were genotyped by Transnetyx. Animals were group-housed under standard laboratory conditions and kept on a 12 h day/night cycle (lights on at 7:00 A.M.). Male and female mice (8-12 weeks old) were used for all experiments. Mice were maintained in accordance with the National Institutes of Health's *Guide for the care and use of laboratory animals*. All methods used were preapproved by the Institutional Animal Care and Use Committee Animals at Florida Atlantic University.

RNAscope ISH. Mice ($n = 2$/genotype and sex) were killed by rapid decapitation, the brain was readily extracted, snap frozen in isopentane chilled with dry ice, and stored at −80°C. Tissues were then frozen in O.C.T. (Sakura Finetek), and 15 μm coronal cryosections of the striatum were collected on Superfrost Plus microscope slides (Thermo Fisher Scientific) and stored at −80°C until use. ISH was performed using the RNAscope Fluorescent Multiplex Reagent Kit (Advanced Cell Diagnostics, #320851), that allows detection of target mRNA at single-cell level. Probes for mouse *Gng7* (Mm-Gng7 #463511), *Drd1* (Mm-Drd1a #406491-C2), and *Drd2* (Mm-Drd2 #406501-C3) were designed and provided by the manufacturer and the experimental procedure followed the manufacturer's instructions. Probes were assigned the following fluorophore configuration: C1-Gng7-Alexa-488, C2-Drd1-Atto-550, and C3-Drd2-Atto-647. DAPI was used for nuclear counterstaining. Positive and negative control probes were used to confirm preservation of sample mRNA and establish nonspecific labeling. Images were acquired using a 20× objective (CFI Plan Apo, Nikon) and Nikon Elements capture software on a Nikon A1R confocal microscope in the FAU Brain Institute Cell Imaging Core. All of the images directly compared were collected using the same laser intensities for the corresponding color channels.

Histology. Eight- to 10-week-old ($n = 3 \times$ genotype $\times$ sex) were anesthetized by Euthasol (Virbac) and transcardially perfused with 4% PFA in PBS. Brains were dissected and postfixed in 4% PBS-PFA overnight, and stored in 30% PBS-sucrose solution for cryoprotection for 3-5 d. Tissues were then frozen in O.C.T. (Sakura Finetek). Tissue sections (30 μm) were prepared using a cryostat (Leica Biosystems) and stored in PBS at 4°C or in antifreeze solution at −20°C for long-term storage. Immunofluorescent staining was performed on sagittal and coronal brain sections containing the striatum, external (eGP) and internal (iGP) globus pallidus, or the substantia nigra pars reticulata (SNpr) as described previously (Ozawa et al., 2015). Sections were blocked with 5% PBS-normal donkey serum and 0.3% Triton X-100 (NDST) for 1 h at room temperature and incubated overnight at 4°C with primary antibody against $G\alpha_{olf}$ (1:1000), μ-opioid receptor (MOR, guinea pig polyclonal, 1:150, Neuromics #GP10106) or DARPP-32 (rabbit polyclonal, 1:100, US Biologicals, #d1075-01). The following day sections were washed 3 times with 1% NDST and incubated for 2 h at room temperature with secondary donkey anti rabbit-IgG Alexa Fluor 488 antibody (1:500, Jackson ImmunoResearch Laboratories # 711-545-152) or anti guinea pig-IgG Alexa Fluor 647 antibody (1:200, Jackson ImmunoResearch Laboratories # 706-605-148). Sections were washed 3 times in PBS and mounted with Fluoromount-G (Southern Biotechnology). Images were acquired on a Nikon A1R confocal microscope in the FAU Brain Institute Cell Imaging Core using either 4× or 10× objectives (CFI Plan Apo, Nikon) and Nikon Elements capture software. Fiji (National Institute of Health) was used to measure the mean fluorescence intensity of $G\alpha_{olf}$ and MOR immunoreactivity in striatal sections, by an experimenter blinded to animal genotypes. To measure $G\alpha_{olf}$ fluorescence intensity in the striatum, the ROI was manually drawn around the dorsal striatum with freehand line tool and $G\alpha_{olf}$ immunoreactivity was measured using ROI manager. Measurements

were averaged from both hemispheres of four rostrocaudal sections per animal (from AP 1.4 mm to +0.2 mm relative to bregma). $G\alpha_{olf}$ immunoreactivity of $Gng7^{fl/fl}D1Cre^{+}$ and $Gng7^{fl/fl}D2Cre^{+}$ were represented as percentage of $Gng7^{fl/fl}$ control group. $G\alpha_{olf}$ fluorescence intensity in striosome and matrix compartments was measured in $G\alpha_{olf}$/MOR double stained striatal sections, from three striatal fields each mouse (AP 1.4, 1.0, and 0.6). The ROI was manually drawn with freehand line tool around the striosomes identified by MOR-positive staining in each section. To measure immunoreactivity in the matrix compartment, the same ROIs were moved to a MOR-negative area. $G\alpha_{olf}$ and MOR fluorescence intensities were measured using ROI manager. Only striosomes whose MOR immunoreactivity was at least 30% over the values of the matrix compartment were considered for analysis.

Membrane preparation. Mice ($n = 5 \times$ genotype $\times$ sex) were killed with an intraperitoneal injection of 100 mg/kg Euthasol (Virbac), and brains were rapidly extracted and rinsed in ice-cold 1× PBS. The brains were then placed in a chilled brain matrix, and 1-mm-thick coronal slices were made using razor blades. Dorsal striatum and nucleus accumbens were dissected out using a fine forceps from two coronal sections (AP 1.7 mm to AP −0.3 mm, relative to bregma, according to Paxinos and Franklin, 2001) and snap frozen in liquid nitrogen. Frozen striatal punches were homogenized on ice with a motorized pestle (Kimble Chase) in HME with proteinase inhibitors (20 mM HEPES, pH 8.0, 2 mM $MgCl_2$, 1 mM EDTA, cOmplete, EDTA-free protease inhibitor cocktail) and then repeatedly passed through a 25-gauge needle on ice. Nuclei and unbroken cells were pelleted by low-speed centrifugation ($350 \times g$) for 5 min, and crude membranes were collected by ultracentrifugation at $250{,}000 \times g$ at 4°C for 30 min, resuspended in 300 μl HME with proteinase inhibitors, aliquoted, and then stored at −80°C until use. The protein concentrations of membrane extracts were determined by Pierce 660 nm Protein Assay Reagent (Thermo Fisher Scientific).

Western blot analysis of striatal membranes. Equal amounts of proteins (25 μg/well) were loaded onto 12% Nu-PAGE Bis-Tris gels (Invitrogen, Thermo Fisher Scientific) and transferred to PVDF membranes (Bio-Rad). Total protein staining was determined using REVERT total protein stain (LI-COR Biosciences) and used as loading control. After 20 min blocking with 10% milk in TBS with 0.01% Tween 20 (TBST), the blots were incubated overnight in 3% milk-TBST with various dilutions of the following antibodies: rabbit polyclonal anti-γ_7 (1:500) (Schwindinger et al., 2003), rabbit polyclonal anti-α_{olf} (1:4000; a gift from Denis Herve) (Corvol et al., 2001), mouse monoclonal anti-AC5 (1:3000; a gift from Kirill Martemyanov) (Xie et al., 2015), rabbit polyclonal anti-γ_3 (1:1000) (Schwindinger et al., 2012), rabbit polyclonal anti-α_s (1:1000, a gift from Catherine Berlot) (Schwindinger et al., 2003), and rabbit polyclonal anti-α_o (1:500) (Schwindinger et al., 2003). After three successive washes with TBST, the blots were incubated for 2 h in 3% milk-TBST with HRP-conjugated goat anti-rabbit or anti-mouse secondary antibodies (1:10,000, Jackson ImmunoResearch Laboratories, #111-035-003 and #111-036-003, respectively). Western blots were visualized and quantitated by enhanced chemiluminescence (Thermo Fisher Scientific) using a LI-COR Odyssey Fc imager.

AC assay. AC activity was determined by incubating membrane protein (1 μg) at 30°C for 10 min in 50 μl of buffer containing 50 mM HEPES, pH 8.0, 0.6 mM EDTA, 100 mg/ml BSA, 100 mM 3-isobutyl-1-methylxanthine, 3 mM phosphoenolpyruvate potassium, 10 mg/ml pyruvate kinase, 5 mM $MgCl_2$, 100 mM adenosine triphosphate, and 10 mM guanosine triphosphate (Xie et al., 2015). Membranes were stimulated with 10 μM forskolin (FSK, Tocris Bioscience, #1099), 25 μM D1R agonist SKF 83822 (Tocris Bioscience, #2075), or 25 μM A2AR agonist CGS 21680 (Tocris Bioscience, #1063). Reactions were stopped by adding an equal volume of 0.2 N HCl. Levels of cAMP were determined by the Direct cAMP ELISA kit according to the manufacturer's protocol (Enzo Life Sciences). Plate absorbance was recorded at 405 nm on a Clariostar instrument (BMG Labtech), and data are expressed as pmol/mg/min.

Behavioral assays. Behavioral testing was performed in the Neurobehavior Core facility of the Florida Atlantic University Brain Institute. Age- (8-12 weeks old) and sex-matched $Gng7^{fl/fl}D1Cre^{+}$ or $Gng7^{fl/fl}D2Cre^{+}$ and respective $Gng7^{fl/fl}$ littermate controls were used for all experiments. Animals were handled and habituated to injection procedure by saline intraperitoneal administration for 3 d preceding the experiment. Mice were habituated for 2 h to the testing room the day before testing and at least 30 min before the start of the experiment. Male and female mice were tested on separate days by an experimenter blinded to animal genotypes.

Accelerating rotarod. Mice were tested for motor skill learning on the accelerating rotarod (Med Associates). Mice were placed on a rod rotating at 4 rpm. Each trial started with 4-40 rpm acceleration rod rotation over 300 s and ended when the mouse fell off the rod, completed a full revolution while hanging onto the rod, or reached 300 s. Latency to fall or to give up walking on the rod was recorded for each trial. Mouse performances were evaluated from three trials per day over 3 d, for a total of 9 trials per mouse. A resting time of 300 s was allowed between each trial.

Grip strength. Grip strength was assessed using a digital grip strength meter (Ametex-Chatillon). Mice were placed on the grip strength apparatus and allowed to grasp a horizontal metal bar with their fore paws while suspended by the tail. The animals were slowly pulled away until they release the handle. The bar was attached to a force transducer, and the peak force produced during the pull on the bar was measured. Grip strength measurements (in gram of force) were averaged across three trials. A resting time of 300 s was allowed between each trial.

Open field locomotor activity. Spontaneous and drug-induced locomotor activity was measured using Med Associates activity chambers. The open field arenas ($27.3 \times 27.3 \times 20.3$ cm) were enclosed within sound-attenuating cubicles that were equipped with a fan for ventilation, white noise to mask extraneous sounds, and two lights. Locomotor activity was detected using a photocell-based automated monitoring system. Horizontal activity was detected by two infrared arrays in the x and y axes and recorded as distance traveled in 5 min intervals. Vertical activity was detected by a third array at 4 cm above the arena floor and measured as number of rearing in 5 min intervals. Med Associates Open Field Activity software was used to track and analyze the mouse movements. Spontaneous locomotor activity was measured for 2 h on first exposure to the open field arena. To assess drug-induced hyperlocomotion, mice were first habituated to the open field arena as described above. On day 2, spontaneous activity was recorded for 30 min, then mice received an injection of saline or appropriate vehicle, and their activity was recorded for additional 90 min. On day 3, mice underwent the same protocol as day 2, but they were administered a dose of drug. Cumulative distance traveled during the 90 min after injection on both days 1 and 2 were considered for data analysis. For morphine induced-locomotor activity, 120 min cumulative distance on days 2 and 3 was analyzed. Drugs were injected at the indicated doses and obtained from the following vendors: D1R agonists SKF 83822 (0.4 mg/kg), SKF 83859 (0.4 mg/kg), and A2AR antagonist SCH 58261 (3 mg/kg) were purchased from Tocris Bioscience, caffeine (30 mg/kg) and D-amphetamine hemisulfate (2.5 mg/kg, free base) were purchased from Sigma-Aldrich, while morphine sulfate (10 mg/kg, free base) was provided by the National Institute of Drug Abuse Drug Supply Program (RTI International). Caffeine, D-amphetamine, and morphine were dissolved in sterile 0.9% saline solution. SKF 83822, SKF 83859, and SCH 58261 were dissolved in 0.2% DMSO and saline. All drugs and respective vehicle or saline solution were injected intraperitoneally in a volume of 5 ml/kg.

Western blot analysis of in vivo *protein phosphorylation.* Three days following handling and habituation to injection procedure, mice ($n = 3\text{-}5 \times$ genotype $\times$ sex) were injected intraperitoneally with saline or D-amphetamine (10 mg/kg) and killed by decapitation at 20 min after injection.

In a second series of experiments, mice ($n = 3\text{-}4 \times$ genotype $\times$ sex) were treated with the acetylcholinesterase inhibitor donepezil (3 mg/kg, i.p., Tocris Bioscience) or saline 10 min before an intraperitoneal injection of D-amphetamine (10 mg/kg) or saline and killed by decapitation at 20 min after injection.

The heads were immersed in liquid nitrogen for 6 s, then the brains were rapidly dissected and placed on an ice-cold brain matrix. Striatal tissues were dissected out as described above, snap frozen in liquid nitrogen, and stored at −80°C until use. Striatal tissues were sonicated in 1% SDS and Halt protease and phosphatase inhibitor cocktail (Thermo

Fisher Scientific) and boiled for 10 min. Protein concentrations of each sample were determined by Pierce 660 nm Protein Assay Reagent. Equal amounts of protein (50 μg/well) were loaded onto 12% Nu-PAGE Bis-Tris gels and transferred to PVDF membranes. After blocking, the blots were incubated overnight in 3% milk-TBST with various dilutions of the following phospho-antibodies: rabbit monoclonal anti-phosphoGluR1-Ser845 (1:1000, Cell Signaling Technology, #8084), mouse monoclonal anti-phosphoERK1/2-Thr202/Tyr204 (1:1000, Cell Signaling Technology, #9106), and rabbit monoclonal anti-phospho-ribosomal protein S6-Ser235/236 (rpS6, 1:1000, Cell Signaling Technology, #4858).The corresponding nonphosphorylated proteins were detected after stripping with Restore stripping buffer (Thermo Fisher Scientific) for 15 min at 37°C and extensive washing in TBS. The following non–phospho-antibodies were used: rabbit monoclonal anti-GluR1 (1:2000, Cell Signaling Technology, #13185), rabbit polyclonal anti-ERK1/2 (1:2000, Cell Signaling Technology, #9102), and rabbit monoclonal anti-S6 ribosomal protein (1:2000, Cell Signaling Technology, #2217). Actin staining was determined using HRP-conjugated rabbit monoclonal anti-β actin antibody (1:10,000, Sigma-Aldrich, #4970) and used as a loading control. Antibody binding was revealed using HRP-conjugated goat anti-rabbit or goat anti-mouse secondary antibodies (1:10,000, Jackson ImmunoResearch Laboratories, ##111-035-003 and #111-036-003, respectively) and the enhanced chemiluminescence detection system. Blots were visualized and quantitated using a LI-COR Odyssey Fc imager.

Statistical analysis. All statistical analyses were performed using GraphPad Prism 8 (GraphPad Software) and Statistica software (version 13.3). Data are expressed as mean ± SEM. *n* refers to the number of independent measures. *p* values ≤ 0.05 were considered to be statistically significant. All studies involved balanced groups of male and female mice; and data from each sex were analyzed separately, except where noted. Parametric statistics were used based on normal distribution of the data, as confirmed by the Shapiro–Wilk test. Student's unpaired, two-tailed *t* test was used to compare protein content in striatal membranes and basal locomotor activity between two genotypes. One-way ANOVA followed by Tukey's *post hoc* test was used to compare striatal $G\alpha_{olf}$ immunoreactivity between different genotypes. Data containing two variables (e.g., genotype factor and treatment) were analyzed by means of two-way ANOVA followed by Tukey's multiple comparison test, when appropriate. Repeated-measures two-way ANOVA was used to analyze locomotor responses to different drugs and $G\alpha_{olf}$-MOR immunoreactivity in the striosome/matrix compartment (with genotype as between-factor and treatment or immunoreactivity in striosome vs matrix as within-factor). Rotarod data and Western blot analysis of protein phosphorylation that included three variables (e.g., genotype, trial, day or pretreatment, treatment and genotype) were analyzed by means of three-way ANOVA.

Results

Characterization of conditional Gγ_7 protein KO mice

Global deletion of *Gng7* mice revealed that loss of G-protein γ_7 disrupts the ordered assembly of a striatal-specific $G\alpha_{olf}\beta_2\gamma_7$ heterotrimer (Schwindinger et al., 2003, 2010). To understand the specific role of the $G\alpha_{olf}\beta_2\gamma_7$ signaling pathway in the two main cell populations of the striatum, we generated new mouse models in which *Gng7* is conditionally deleted either in D_1R- or D_2R-expressing MSNs. To determine the specificity and extent of this deletion, DNA was isolated from either $Gng7^{fl/fl}D_1Cre^+$ or $Gng7^{fl/fl}D_2Cre^+$ mice and analyzed by PCR. Among the various brain regions, conditional deletion of the *Gng7* gene occurred to the greatest degree in the striatum. However, recombination also occurred in other brain regions, including the PFC, hippocampus, and midbrain (Fig. 1*A*), as expected based on regional distributions of D_1R and D_2R. To verify that the *Gng7* gene was specifically ablated in distinct populations of MSNs, we also used ISH (Fig. 1*B*). As expected, γ_7 mRNA was abundantly expressed in both D_1R- and D_2R-MSNs throughout the striatum of WT mice (Fig. 1*Ba–Be*). As first reported by Watson et al. (1994), the γ_7 mRNA fluorescence signal was clustered in neuronal cell bodies, whereas diffused and punctuated staining pattern was detected around the soma, confirming a dendritic localization of the γ_7 mRNA. Validating the conditional nature of the gene-targeted deletion, the γ_7-positive mRNA signal was strongly reduced in either D_1R- or D_2R-expressing MSNs visualized from striatal sections of $Gng7^{fl/fl}D_1Cre^+$ (Fig. 1*Bf–Bj*) and $Gng7^{fl/fl}D_2Cre^+$ mice (Fig. 1*Bk–Bo*), respectively. Interestingly, in striatal sections from $Gng7^{fl/fl}$ and $Gng7^{fl/fl}D_1Cre^+$ mice, we observed that γ_7 mRNA was virtually absent in a few large-sized D_2R-expressing neurons, which may represent a subpopulation of D_2R-expressing cholinergic interneurons (Fig. 1*C*).

Global loss of γ_7 suppressed the levels of $G\alpha_{olf}$ protein without affecting mRNA level of the *Gnal* transcript (Schwindinger et al., 2003). To further extend these findings, we used immunohistochemistry to assess $G\alpha_{olf}$ protein expression in the striatum and along the axonal projections of D_1R- and D_2R-positive MSNs that track to the globus pallidus internus (GPi)/substantia nigra pars reticulata (SNr) and globus pallidus externus (GPe), respectively (Figs. 2 and 3). $G\alpha_{olf}$ immunoreactivity was highly concentrated in the dorsal striatum with the characteristic matrix-striosome distribution pattern (Ruiz-DeDiego et al., 2015; Crittenden et al., 2016), as evidenced by heightened $G\alpha_{olf}$ immunolabeling colocalizing with striosomal marker MOR staining (Fig. 2*Aa–c,f–h,k–m*). Positive $G\alpha_{olf}$ immunolabeling was detected in the ventral striatum and olfactory tubercle but was relatively absent in the cerebral cortex (Fig. 3*A,C,E*). We also confirmed decreased $G\alpha_{olf}$ immunoreactivity in the dorsal striatum of both conditional KO lines (overall ANOVA $F_{(2,15)} = 15.11$, $p < 0.001$; *post hoc* analysis: $Gng7^{fl/fl}D_1Cre^+$ ($p < 0.001$), and $Gng7^{fl/fl}D_2Cre^+$, $p < 0.05$; Fig. 2*Ba*). Likewise, ANOVA of $G\alpha_{olf}$ immunoreactivity in the striosome and matrix compartments revealed a significant effect of "genotype" ($F_{(2,15)} = 5.4$, $p < 0.05$) and "compartment" ($F_{(1,15)} = 97.45$, $p < 0.001$), as well as a significant "genotype × compartment" interaction ($F_{(2,15)} = 5.8$, $p < 0.05$). In this regard, Tukey's *post hoc* analysis showed that the $G\alpha_{olf}$ striosomal expression pattern was significantly reduced in striatal sections from $Gng7^{fl/fl}D_1Cre^+$ mice but was preserved in $Gng7^{fl/fl}D_2Cre^+$ mice (Fig. 2*Bb*). Attesting to the specificity of this effect, immunostaining of the striosomal marker MOR did not change among genotypes (Fig. 2*Bc*).

Consistent with known neurocircuitry and conditional nature of the KOs, drastic loss of $G\alpha_{olf}$-positive MSNs with axonal projections to the GPi/SNr was observed in sections from $Gng7^{fl/fl}D_1Cre^+$ mice (Figs. 2*Ai* and 3*C*), whereas selective reduction of $G\alpha_{olf}$ immunoreactive signal in the GPe was evident in sections from $Gng7^{fl/fl}D_2Cre^+$ mice (Figs. 2*An* and 3*E*). In contrast, DARPP-32 staining was preserved in the striatum and axonal projections of both conditional KO mouse strains, indicating maintenance of striatal and axonal projection integrity (Fig. 3*B,D,F*).

Extending the immunostaining results, immunoblot analysis of striatal membranes from $Gng7^{fl/fl}D_1Cre^+$ mice confirmed marked reduction of the γ_7 protein compared with membranes from $Gng7^{fl/fl}$ controls in both male and female mice (males: $t_{(8)} = 5.9$, $p < 0.001$; females: $t_{(8)} = 9.9$, $p < 0.001$; Fig. 4*A,B*). Along with loss of γ_7 protein, there was a coordinated decrease in the $G\alpha_{olf}$ protein in $Gng7^{fl/fl}D_1Cre^+$ mice (males: $t_{(8)} = 7.8$, $p < 0.001$; females: $t_{(8)} = 2.8$, $p < 0.05$; Fig. 4*A,B*), consistent with reduction of both γ_7 and $G\alpha_{olf}$ in approximately half of MSNs. Similarly, $Gng7^{fl/fl}D_2Cre^+$ male and female mice showed lowered γ_7 (males: $t_{(8)} = 5.2$, $p < 0.001$; females: $t_{(8)} = 2.4$, $p < 0.05$; Fig. 4*C,D*) and $G\alpha_{olf}$ protein levels (males: $t_{(8)} = 3.3$, $p < 0.05$; females: $t_{(8)} = 3.2$, $p < 0.05$; Fig. 4*C,D*) compared with $Gng7^{fl/fl}$

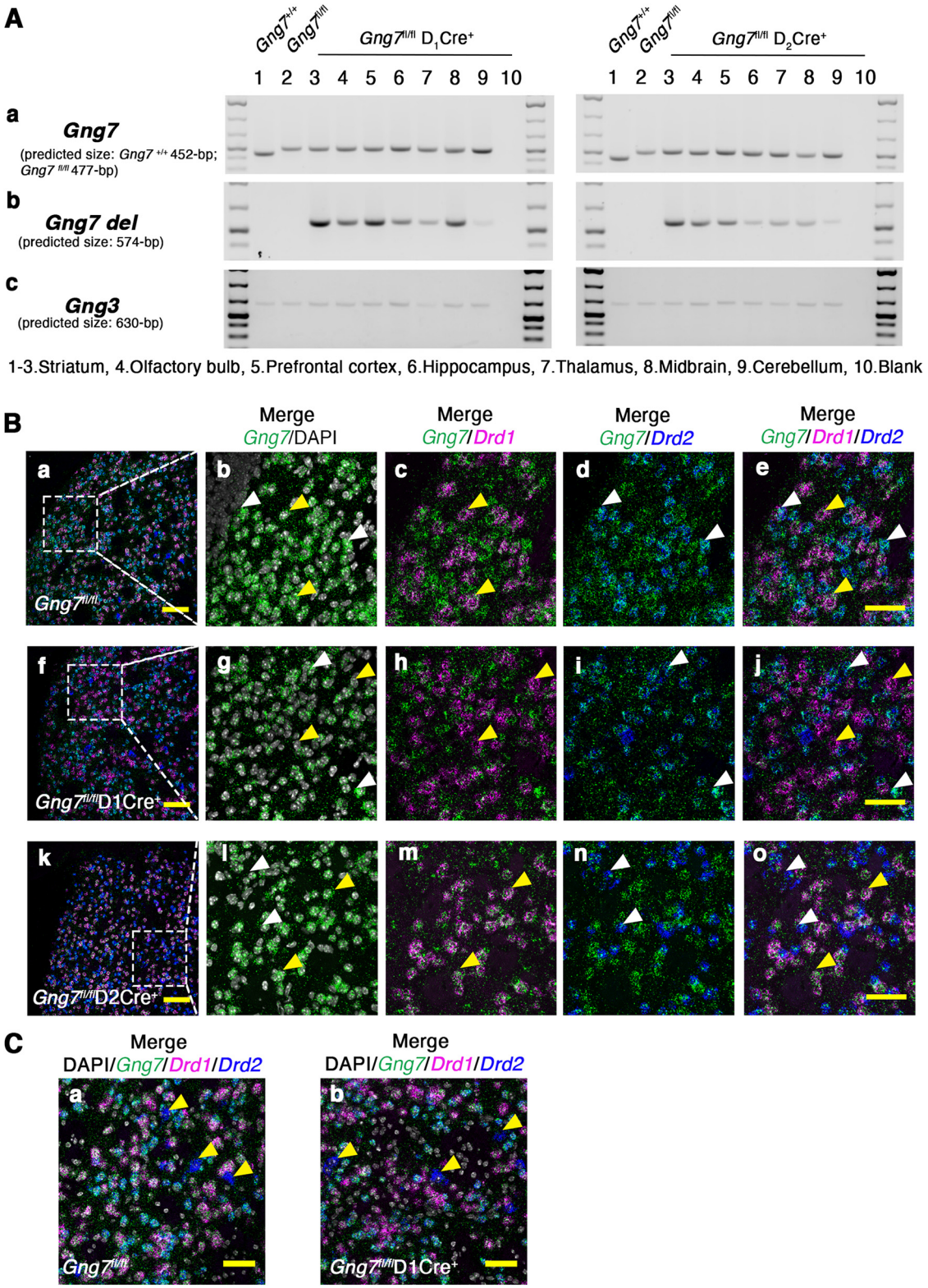

Figure 1. Molecular characterization of conditional D_1R- and D_2R-γ_7 KO mice. ***A***, Genotype PCR products for the WT, floxed (***Aa***) and deleted (***Ab***) *Gng7* allele in brain regions of $Gng7^{+/+}$, $Gng7^{fl/fl}$, $Gng7^{fl/fl}D_1Cre^+$, and $Gng7^{fl/fl}D_2Cre^+$ mice. PCR products for the *Gng3* allele were used as loading control (***Ac***). The *Gng7* gene is expressed across multiple brain regions, including the striatum, olfactory bulb, hippocampus, PFC, thalamus, midbrain, and cerebellum. D_1Cre- or D_2-Cre-mediated recombination of the floxed allele is high in the striatum of both $Gng7^{fl/fl}D_1Cre^+$ and $Gng7^{fl/fl}D_2Cre^+$ mice. However, recombination also occurs in the olfactory bulb, hippocampus, PFC, midbrain, and to a very low extent in the thalamus and cerebellum. ***B***, Triple fluorescence RNAscope ISH probing γ_7 (*Gng7*, green label), D_1R (*Drd1*, magenta label), and D_2R (*Drd2*, blu label) mRNAs. DAPI staining (white label) was used to label cell nuclei. Representative images of 20× magnification widefield (***Ba***,***Bf***,***Bk***, merge *Gng7-Drd1-Drd2*-DAPI; scale bar, 100 μm) and zoomed in (3×) images (***Bb–Be***,***Bg–Bj***,***Bl–Bo***; scale bar, 50 μm). In $Gng7^{fl/fl}$ WT mice, γ_7 mRNA colocalized with both D_1R (***Ac*** and ***Ae***, yellow arrows) and D_2R (***Bd***,***Be***, white arrows) mRNAs. In $Gng7^{fl/fl}D_1Cre^+$ mice γ_7-D_1R mRNAs, colocalization was lost (***Bh***,***Bj***, yellow arrows), while colocalization with D_2R mRNA was preserved (***Bd***,***Be***, white arrows). Conversely, $Gng7^{fl/fl}D_2Cre^+$ mice showed almost complete loss γ_7-D_2R mRNAs colocalization (***Bn***,***Bo***, white arrows), while γ_7-D_1R

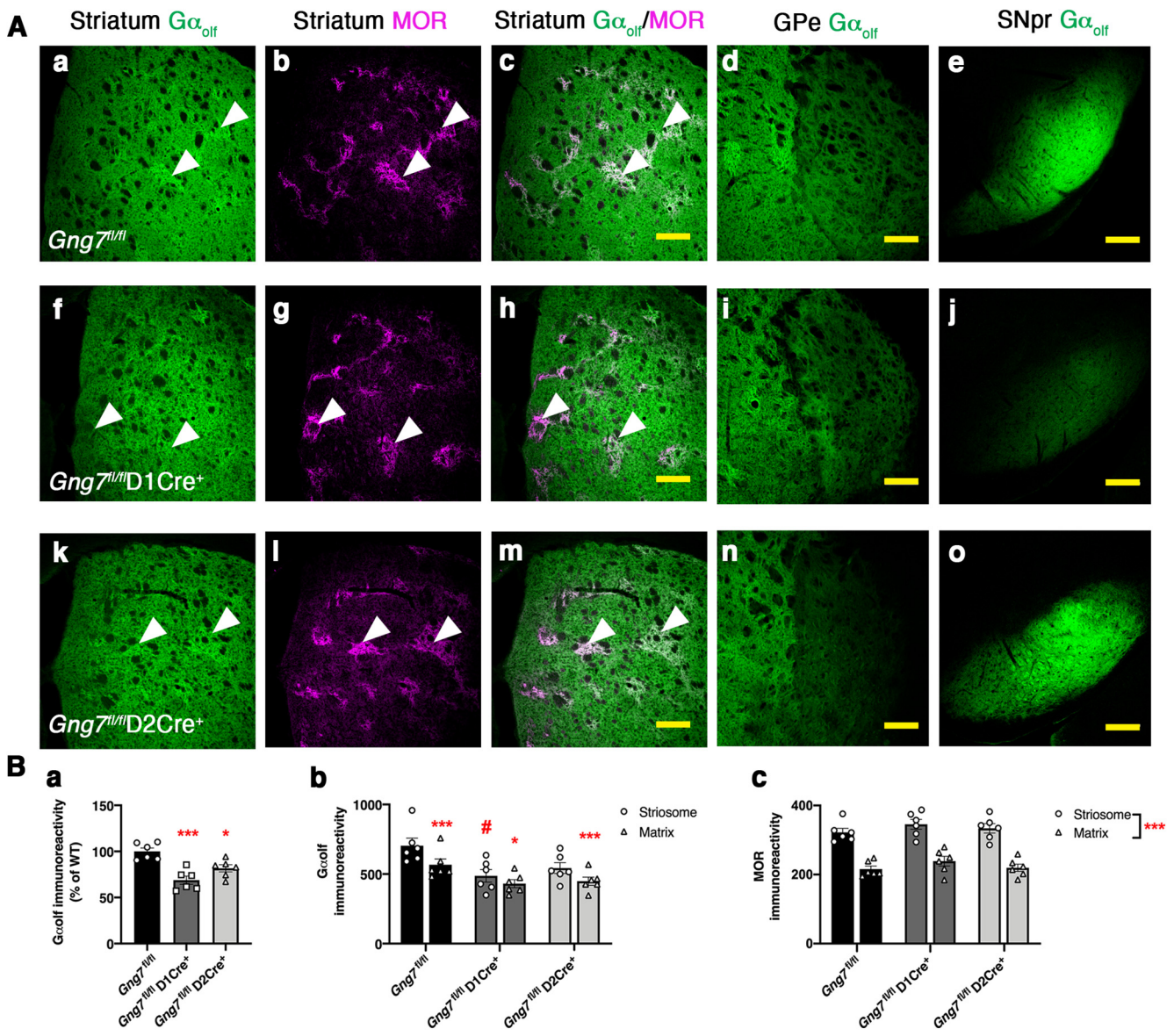

Figure 2. Molecular characterization of conditional D_1R- and D_2R-γ_7 KO mice. ***A***, $G\alpha_{olf}$ and MOR immunofluorescence in brain sections of $Gng7^{fl/fl}$ (***Aa–Ae***), $Gng7^{fl/fl}D_1Cre^+$ (***Af–Aj***), and $Gng7^{fl/fl}D_2Cre^+$ mice (***Ak–Ao***). Scale bar, 200 μm. In $Gng7^{fl/fl}$, $G\alpha_{olf}$ immunoreactivity was found throughout the striatum, highly concentrated in the striosome compartment where it colocalized with MOR (***Aa–Ac***). $G\alpha_{olf}$ labeling was also found in striatal projection areas, including the GP (***Ad***) and the SNpr (***Ae***). Loss of γ_7 causes a drastic reduction of striatal $G\alpha_{olf}$ immunoreactivity in both $Gng7^{fl/fl}D_1Cre^+$ (***Af–Aj***) and $Gng7^{fl/fl}D_2Cre^+$ (***Ak–Ao***) mice. $Gng7^{fl/fl}D_1Cre^+$ mice also exhibited profound loss of $G\alpha_{olf}$-positive terminal in the SNpr (***Aj***), while $G\alpha_{olf}$ fluorescence was selectively reduced in the GP of $Gng7^{fl/fl}D_2Cre^+$ mice (***An***). ***B***, Quantification of immunofluorescence signal for $G\alpha_{olf}$ and MOR in the striatum. $G\alpha_{olf}$ mean intensity fluorescent signal in the dorsal striatum was decreased in both $Gng7^{fl/fl}D_1Cre^+$ and $Gng7^{fl/fl}D_2Cre^+$ mice compared with $Gng7^{fl/fl}$ WTs (***Ba***, one-way ANOVA: $^*p < 0.05$; $^{***}p < 0.001$). The $G\alpha_{olf}$ striosome-matrix distributional pattern was reduced in $Gng7^{fl/fl}D_1Cre^+$ mice but conserved in $Gng7^{fl/fl}D_2Cre^+$ mice. Striosomal MOR staining did not change among genotypes (***Bb***,***Bc***, two-way repeated-measures ANOVA and Tukey's *post hoc*: $^*p < 0.05$; $^{***}p < 0.001$ matrix vs striosome; $^{\#}p < 0.05$ $Gng7^{fl/fl}D_1Cre^+$ striosome vs WT $Gng7^{fl/fl}$ striosome, "genotype × compartment" effect). Data are mean ± SEM. $n = 6$ mice/group.

littermates. Protein levels of $\gamma 3$, $\gamma 2$, $G\alpha_s$, and $G\alpha_o$ did not change among the different genotypes (Fig. 4), confirming the specificity of these effects and further indicating that γ_7 and $G\alpha_{olf}$ cannot be replaced by other γ or α subtypes *in vivo*. Together, these results show that gene-targeted loss of γ_7 in subpopulations of MSNs results in coordinate loss of $G\alpha_{olf}$ and further confirm that γ_7 subunit is required for cell type-specific assembly of a distinct $G\alpha_{olf}\beta_2\gamma_7$ heterotrimer (Schwindinger et al., 2003, 2010).

AC activity in $G\alpha_{olf}$ deficient D_1R- and D_2R-MSNs

It has been demonstrated that the $G\alpha_{olf}\beta_2\gamma_7$ heterotrimer forms complexes with AC Type 5, the main AC isoform in the striatum, and contributes to its stability (Iwamoto et al., 2004; Xie et al., 2015). Quantitative immunoblot analyses revealed that the AC5 protein level was not significantly changed in striatal membranes from $Gng7^{fl/fl}D_2$ Cre^+ male mice ($t_{(8)}$ = 2.09, NS), although a significant reduction was observed in membranes from

←

mRNAs colocalization remained (***Bm***,***Bo***, yellow arrows). ***C***, Representative images of zoomed in (2×) images (merge *Gng7-Drd1-Drd2*-DAPI; scale bar, 50 μm). In $Gng7^{fl/fl}$ WT (***Ca***) and $Gng7^{fl/fl}D_1Cre^+$ mice (***Cb***), a small percentage of *Drd2*-positive neurons (yellow arrows), presumably cholinergic interneurons, does not show colocalization with the γ_7 mRNA.

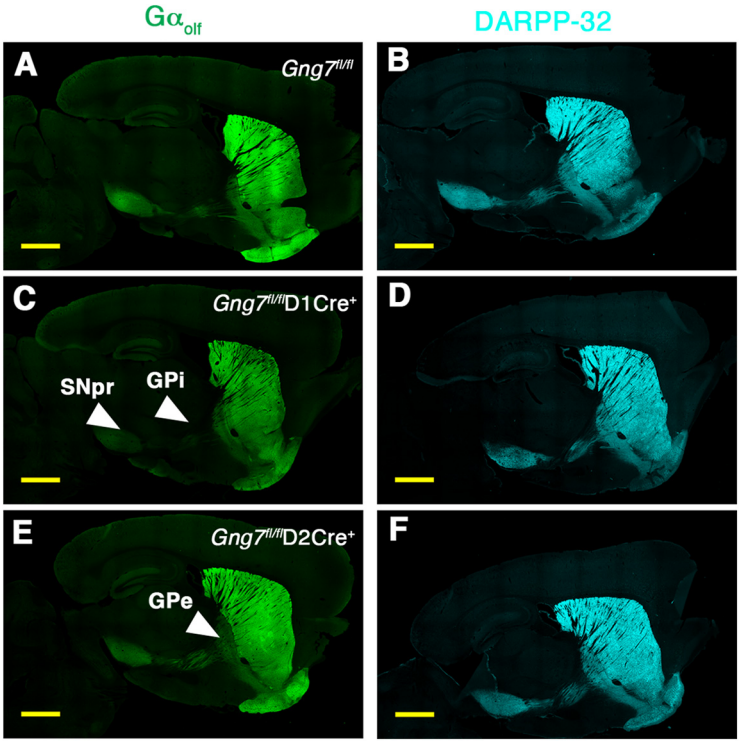

Figure 3. Molecular characterization of conditional D_1R- and D_2R-γ_7 KO mice. Gα_{olf} and DARPP immunofluorescence in sagittal brain sections of Gng7$^{fl/fl}$ (***A***,***B***), *Gng7*$^{fl/fl}$D$_1$Cre$^+$ (***C***,***D***), and *Gng7*$^{fl/fl}$D$_2$Cre$^+$ mice (***E***,***F***). Scale bar, 1 mm. In Gng7$^{fl/fl}$, Gα_{olf} immunoreactivity was found throughout the striatum and in MSN axonal projections to the GPi/SNr and GPe, which are the main target regions for D_1R- and D_2R-positive MSNs, respectively. *Gng7*$^{fl/fl}$D$_1$Cre$^+$ mice exhibited profound loss of Gα_{olf} immunoreactivity in the striatum and striatal projections to the GPi and SNpr (***C***). In *Gng7*$^{fl/fl}$D$_2$Cre$^+$ mice, Gα_{olf} immunoreactivity was reduced in the striatum and striatal projections to the Gpe (***E***). DARPP staining was preserved in the striatum and striatal projection areas in all genotypes (***B***,***D***,***F***).

Gng7$^{fl/fl}$D$_1$Cre$^+$ females ($t_{(8)}$ = 4.5, $p < 0.01$; Fig. 4*A*,*B*). Furthermore, there was no change of AC5 protein content in striatal membranes of either male or female *Gng7*$^{fl/fl}$D$_2$Cre$^+$ mice (males: $t_{(8)}$ = 1.6, NS; females: $t_{(8)}$ = 0.5, NS; Fig. 4*C*,*D*). These results suggest that selective loss of Gα_{olf} signaling components in one population of MSNs is likely not sufficient to alter significantly the levels of AC5. Incubation of striatal membranes with the direct AC activator FSK caused ~3- to 4-fold increase of cAMP levels compared with untreated samples. However, consistent with normal levels of AC5, we did not detect deficits in FSK-stimulated AC activity in striatal membranes of *Gng7*$^{fl/fl}$D$_1$Cre$^+$ (males: main effect of "treatment" $F_{(1,8)}$ = 45.9, $p < 0.001$, "genotype × treatment" interaction $F_{(1,8)}$ = 0.05, NS; females: main effect of "treatment" $F_{(1,8)}$ = 29, $p < 0.001$, "genotype × treatment" interaction $F_{(1,8)}$ = 0.08, NS; Fig. 5*A*,*B*) and *Gng7*$^{fl/fl}$D$_2$Cre$^+$ mice (males: main effect of "treatment" $F_{(1,8)}$ = 30.2, $p < 0.001$, "genotype × treatment" interaction $F_{(1,8)}$ = 0.8, NS; females: main effect of "treatment" $F_{(1,8)}$ = 16.6, $p < 0.001$, "genotype × treatment" interaction $F_{(1,8)}$ = 0.0008, NS; Fig. 5*C*,*D*), compared with corresponding *Gng7*$^{fl/fl}$ littermates. In contrast, we observed that the efficiency of D_1R- and A_{2A}R-coupling to AC was selectively impaired in striatal membranes from *Gng7*$^{fl/fl}$D$_1$Cre$^+$ and *Gng7*$^{fl/fl}$D$_2$Cre$^+$ mice, respectively. Indeed, as shown in Figure 5*E*, *F*, treatment with the D_1R agonist SKF 83822 did not stimulate cAMP production in striatal membranes of male or female *Gng7*$^{fl/fl}$D$_1$Cre$^+$ mice (males: "genotype × treatment" interaction $F_{(1,8)}$ = 5.7, $p < 0.05$; females: "genotype × treatment" interaction $F_{(1,8)}$ = 5.4, $p < 0.05$), whereas the ability of the A_{2A}R agonist CGS 21680 to increase cAMP was unaffected in membranes of both *Gng7*$^{fl/fl}$D$_1$Cre$^+$ and WT mice (males: main effect of "treatment" $F_{(1,8)}$ = 28.6, $p < 0.001$, "genotype × treatment" interaction $F_{(1,8)}$ = 0.2, NS; females: main effect of "treatment" $F_{(1,8)}$ = 126.5, $p < 0.001$, "genotype × treatment" interaction $F_{(1,8)}$ = 0.4, NS).

Conversely, treatment with the A_{2A}R agonist CGS 21680 did not increase cAMP levels in striatal membranes of male or female *Gng7*$^{fl/fl}$D$_2$Cre$^+$ mice (males: "genotype × treatment" interaction $F_{(1,8)}$ = 8.9, $p < 0.05$; females: "genotype × treatment" interaction $F_{(1,8)}$ = 7.2, $p < 0.05$; Fig. 5*G*,*H*), whereas the SKF 83822-stimulated AC activity was preserved in both sexes (males: main effect of "treatment" $F_{(1,8)}$ = 50.7, $p < 0.001$, "genotype × treatment" interaction $F_{(1,8)}$ = 2.1, NS; females: main effect of "treatment" $F_{(1,8)}$ = 25.2, $p < 0.001$, "genotype × treatment" interaction $F_{(1,8)}$ = 1.1, NS; Fig. 5*G*,*H*). Collectively, these findings confirm that striatal Gα_{olf} signaling components are necessary for coupling of D_1R and A_{2A}R to AC, but not required for the stability and function of AC5.

Assessment of motor abilities in conditional Gγ_7 protein KO mice

A coordinated balance of the activities of D_1R- and D_2R-expressing of striatal MSNs is responsible for proper control of movements, whereas a preponderance of function in one MSN subpopulation over the other results in motor abnormalities characteristic of basal ganglia disorders (Albin et al., 1989; Nelson and Kreitzer, 2014). Likewise, compelling evidence supports a role for the Gα_{olf} signaling pathway in the emergence of motor disorders, such as dystonia, in humans and mice (Fuchs et al., 2013; Sasaki et al., 2013; Pelosi et al., 2017). To assess the relative contributions of G$\alpha_{olf}\beta_2\gamma_7$-mediated signaling downstream of either striatal D_1R or A2R activation, we evaluated motor coordination and learning by quantifying performance of conditional KO lines in the accelerated rotarod paradigm. Both male and female mice representing all three genotypes (*Gng7*$^{fl/fl}$D$_1$ Cre$^+$, *Gng7*$^{fl/fl}$D$_2$ Cre$^+$, and *Gng7*$^{fl/fl}$ mice) improved their ability to stay on the rod with each subsequent trial and day, and there were no genotype differences in rotarod performance (Fig. 6*A*–*D*). Consistently, no impairments of neuromuscular function were observed as measured by performance on the grip strength test (Fig. 6*E*,*F*).

To determine the relative roles of striatal D_1R- and A_{2A}R-mediated G$\alpha_{olf}\beta_2\gamma_7$ signal on spontaneous locomotor activity, *Gng7*$^{fl/fl}$D$_1$Cre$^+$ and *Gng7*$^{fl/fl}$D$_2$Cre$^+$ mice were tested for exploratory activity on first exposure to an open field arena. *Gng7*$^{fl/fl}$D$_1$Cre$^+$ mice showed no changes in locomotor behavior (males: $t_{(32)}$ = 0.7, NS; females: $t_{(36)}$ = 0.8, NS; Fig. 6*G*,*H*), vertical activity, stereotypy, or thigmotaxis compared with WTs (Table 1). In contrast, *Gng7*$^{fl/fl}$D$_2$Cre$^+$ mice exhibited marked hyperactivity on exposure to a novel environment as compared with WTs (males: $t_{(31)}$ = 5.8, $p < 0.001$; females: $t_{(29)}$ = 4.8, $p < 0.001$; Fig. 6*I*, *J*), although habituation to the arena was normal, as evidenced by a progressive attenuation of locomotor activity over the 2 h

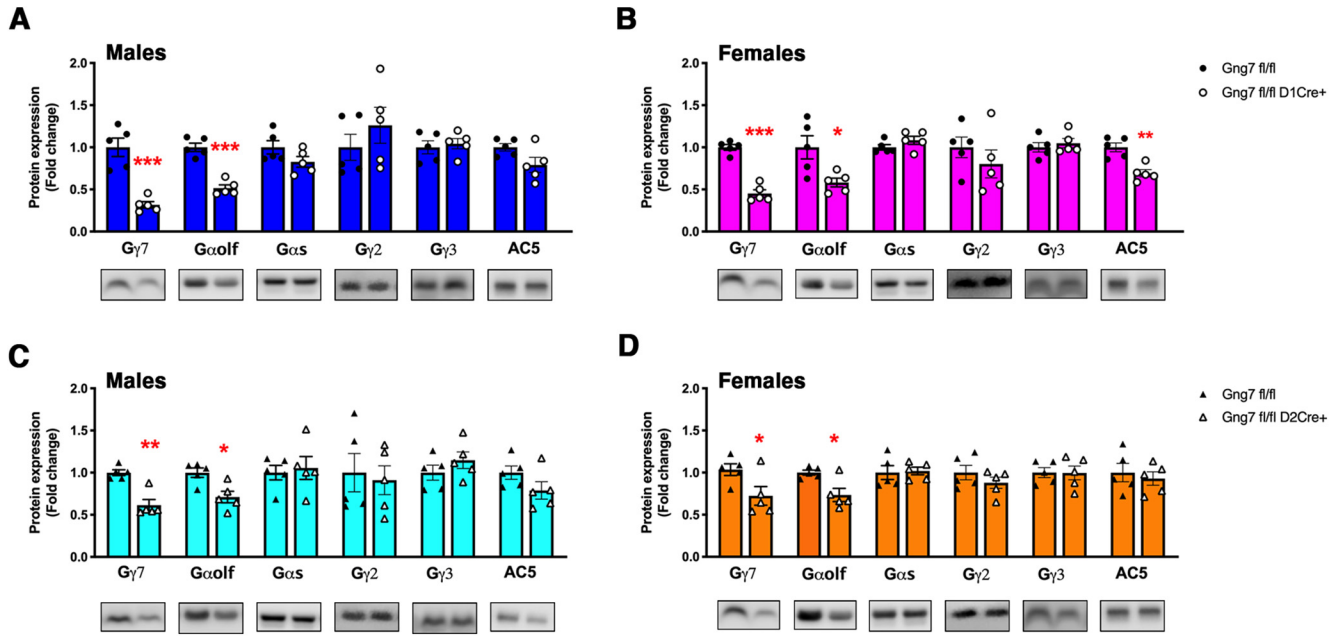

Figure 4. Molecular characterization of conditional D_1R- and D_2R-γ_7 KO mice. Representative immunoblot data and quantification of γ_7, $G\alpha_{olf}$ $G\alpha_{s,}$ γ_2, γ_3 and AC5 protein levels in striatal membranes of male and female $Gng7^{fl/fl}D_1Cre^+$ (***A,B***) and $Gng7^{fl/fl}D_2Cre^+$ mice (***C,D***). Each column represents a normalized ratio (fold-change) relative to total protein loading and to controls ($Gng7^{fl/fl}$). Western blot analysis confirmed that loss of γ_7 caused a reduction of striatal $G\alpha_{olf}$ protein levels in both conditional KO mouse lines. AC5 protein was substantially preserved, although a significant reduction of AC5 protein levels was observed in $Gng7^{fl/fl}D_1Cre^+$ female mice (***B***). Loss of γ_7 did not cause compensatory changes of striatal $G\alpha_s$, γ_3, and γ_2 protein levels in both conditional KO mouse lines. $^*p < 0.05$, $^{**}p < 0.01$, $^{***}p < 0.001$, $Gng7^{fl/fl}D_1Cre^+$ or $Gng7^{fl/fl}D_2Cre^+$ compared with $Gng7^{fl/fl}$ WT littermates (Student's *t* test). Data are mean ± SEM. $n = 5$ mice/group.

session. Suggesting that the hyperlocomotive phenotype was not exclusively related to novelty, the elevated locomotor activity of $Gng7^{fl/fl}D_2Cre^+$ mice was observed over multiple exposures to the open field arena, particularly during the first 30 min of a 2 h open field test (unpublished observation). Vertical activity and stereotypic behavior were also enhanced compared with $Gng7^{fl/fl}$ WTs. In contrast, thigmotaxis was unaltered, indicating that hyperlocomotion was likely not associated with changes in anxiety-like behavior (Table 1). Finally, validating these effects were related to cell type-specific loss of $G\alpha_{olf}\beta_2\gamma_7$ signal, locomotor activities were unchanged in both D_1Cre^+ and D_2Cre^+ mice compared with controls (males D1Cre: $t_{(15)} = 1.1$, NS; females D1Cre: $t_{(13)} = 0.1$, NS; males D2Cre: $t_{(21)} = 0.9$, NS; females D2Cre: $t_{(17)} = 0.2$, NS; Fig. 6*K*). Together, these results demonstrate that $G\alpha_{olf}\beta_2\gamma_7$-mediated signaling downstream of either striatal D_1R- or $A_{2A}R$-activation is dispensable for motor coordination and grip strength. Surprisingly, loss of $G\alpha_{olf}\beta_2\gamma_7$-mediated signaling in D_1R-expressing MSNs had little or no effect on spontaneous locomotor activity, whereas reciprocal deletion of $G\alpha_{olf}\beta_2\gamma_7$-mediated signaling in D_2R-expressing MSNs produced a dramatic increase in locomotor behavior.

Assessment of locomotor responses to D_1R and $A_{2A}R$ directed ligands

While dispensable for spontaneous locomotor behavior, we hypothesized $G\alpha_{olf}\beta_2\gamma_7$-mediated signaling in D_1R-MSNs may assume greater importance in regulating locomotor activity under conditions in which D_1R is selectively stimulated. To test this possibility, we compared locomotor responses of $Gng7^{fl/fl}D_1Cre^+$ mice and WT littermates to the administration of two distinct D_1R agonists, SKF 83822 and SKF 83959, that reportedly exhibit different efficacies for cAMP production and phosphatidylinositol turnover (Undie et al., 1994; Jin et al., 2003; O'Sullivan et al., 2008). Injection of mice with either SKF 838222 (0.4 mg/kg, i.p.; Fig. 7*A*) or SKF 83959 (0.4 mg/kg, i.p.; Fig. 7*B*) caused equivalent psychomotor responses in male and female $Gng7^{fl/fl}D_1Cre^+$ mice compared with controls. Two-way ANOVA revealed a significant effect of either SKF 38222 or SKF 83959 treatments, but no "genotype × treatment" interaction effect of genotype (SKF 838222 males: main effect of "treatment" $F_{(1,14)} = 87.6$, $p < 0.001$, "genotype × treatment" interaction $F_{(1,14)} = 0.04$, NS; SKF 838222 females: main effect of "treatment" $F_{(1,13)} = 78.6$, $p < 0.001$, "genotype × treatment" interaction $F_{(1,13)} = 0.9$, NS; SKF 83959 males: main effect of "treatment" $F_{(1,12)} = 42.9$, $p < 0.001$, "genotype × treatment" interaction $F_{(1,12)} = 4.1$, NS; SKF 83959 females: main effect of "treatment" $F_{(1,12)} = 73.2$, $p < 0.001$, "genotype × treatment" interaction $F_{(1,12)} = 0.07$, NS). Together, these results suggest that $G\alpha_{olf}\beta_2\gamma_7$ heterotrimer signaling in D_1R-MSNs is not responsible for locomotor stimulating responses of D_1R agonists and may indicate the involvement of D_1R-mediated signaling pathways other than cAMP for the regulation of locomotor behavior.

Subsequently, we examined the contribution of $A_{2A}R$-$G\alpha_{olf}\beta_2\gamma_7$-cAMP signaling in D_2R-expressing neurons by testing the locomotor enhancing effects of the nonselective $A_1/A_{2A}R$ antagonist caffeine (30 mg/kg, i.p.) on $Gng7^{fl/fl}D_2$ Cre^+ mice and control littermates. In agreement with our previous observation in global γ_7 KO mice (Schwindinger et al., 2010), $Gng7^{fl/fl}D_2Cre^+$ male mice showed an attenuated response to caffeine (Fig. 7*C*). Two-way ANOVA revealed a significant effect of "treatment" ($F_{(1,14)} = 42.8$, $p < 0.001$) and "genotype" ($F_{(1,14)} = 6.0$, $p < 0.05$), as well as a significant "genotype × treatment" interaction ($F_{(1,14)} = 8.2$, $p < 0.05$). Tukey's *post hoc* analysis confirmed that locomotor response to caffeine was reduced in $Gng7^{fl/fl}D_2Cre^+$ males, compared with WTs. Interestingly, however, female $Gng7^{fl/fl}D_2Cre^+$ mice response to caffeine was not significantly different from controls (main effect of "treatment" $F_{(1,14)} = 32.8$, $p < 0.001$), although a trend to reduced caffeine

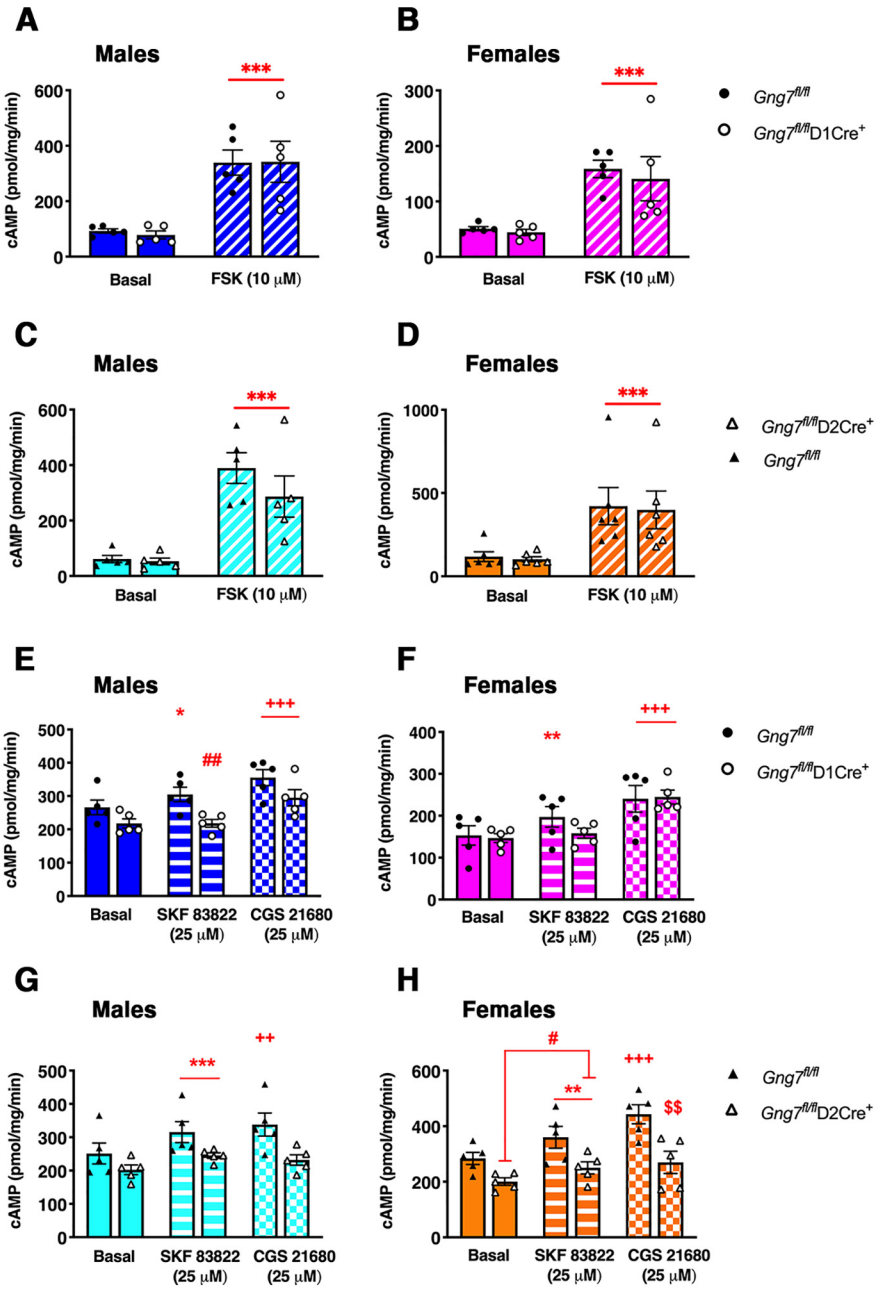

Figure 5. Molecular characterization of conditional D_1R- and D_2R-γ_7 KO mice. AC activity in striatal membranes of male and female *Gng7*$^{fl/fl}$D$_1$Cre$^+$ (***A***,***B***,***E***,***F***), *Gng7*$^{fl/fl}$D$_2$Cre$^+$ mice (***C***,***D***,***G***,***H***), and WT littermates. AC activity was measured under basal conditions (DMSO) or in the presence of 10 μM FSK, 25 μM D_1R agonist SKF 83822, or 25 μM A2AR agonist CGS 21680. AC stimulation by FSK was not significantly different between D_1R- or D_2R-γ_7 KO mice and WT controls (***A–D***, two-way repeated-measures ANOVA: ***$p < 0.001$ basal vs FSK, "treatment" effect). In male and female *Gng7*$^{fl/fl}$D$_1$Cre$^+$ mice, D_1R agonist SKF 83822 did not significantly elevate cAMP levels over the baseline level (***E***,***F***, two-way repeated-measures ANOVA and Tukey's *post hoc*: *$p < 0.05$, **$p < 0.01$, *Gng7*$^{fl/fl}$-basal vs *Gng7*$^{fl/fl}$-SKF 83822; ##$p < 0.01$, *Gng7*$^{fl/fl}$D$_1$Cre$^+$ vs *Gng7*$^{fl/fl}$, "genotype × treatment" effect). Membranes incubation with A2AR agonist CGS21680 caused a significant increase of cAMP levels in both genotypes and sexes (***E***,***F***, two-way repeated-measures ANOVA and Tukey's *post hoc*: $^{+++}p < 0.001$, CGS 21680 vs basal, "treatment" effect). In contrast, AC stimulation with SKF 83822 was preserved in male and female *Gng7*$^{fl/fl}$D$_2$Cre$^+$ mice compared with controls (***G***,***H***, two-way repeated-measures ANOVA: **$p < 0.01$, ***$p < 0.001$, SKF 83822 vs basal, "treatment" effect; #$p < 0.05$, *Gng7*$^{fl/fl}$D$_2$Cre$^+$ vs *Gng7*$^{fl/fl}$, "genotype" effect), while AC stimulation with CGS 21680 was selectively impaired in the conditional KO line (***G***,***H***, two-way repeated-measures ANOVA and Tukey's *post hoc*: $^{++}p < 0.01$, $^{+++}p < 0.001$, *Gng7*$^{fl/fl}$-basal vs *Gng7*$^{fl/fl}$-CGS 21680; $^{\$\$}p < 0.01$, *Gng7*$^{fl/fl}D_2Cre^+$-CGS21680 vs *Gng7*$^{fl/fl}$-CGS21680, "genotype × treatment" effect). Data are mean ± SEM. $n = 5$ mice/group.

locomotor response was observed ("genotype × treatment" interaction $F_{(1,14)} = 4.02$, $p = 0.06$, NS; Fig. 7*C*). Finally, we tested the ability of the selective A_{2A}R antagonist SCH 58261 (3 mg/kg, i.p.) to induce a locomotor activation in *Gng7*$^{fl/fl}$D$_2$Cre$^+$ mice and controls. We found that locomotor responses to SCH 58261 were similar among genotypes and sexes (males: main effect of "treatment" $F_{(1,14)} = 15.1$, $p < 0.01$, "genotype × treatment" interaction $F_{(1,14)} = 0.6$, NS; females: main effect of "treatment" $F_{(1,14)} = 39.9$, $p < 0.001$, "genotype × treatment" interaction $F_{(1,14)} = 0.002$, NS; Fig. 7*D*). Because A_{2A}Rs are highly expressed in MSNs and also localized presynaptically in corticostriatal glutamatergic terminals, the different results obtained with caffeine and SCH 58261 may be related to different presynaptic versus postsynaptic mechanisms of action (Orru et al., 2011). Nevertheless, the diminished psychomotor stimulating effects of caffeine in *Gng7*$^{fl/fl}$D$_2$Cre$^+$ mice confirm an important role for G$\alpha_{olf}\beta_2\gamma_7$-mediated signaling in the striatopallidal circuitry for the regulation of locomotor behavior.

Locomotor responses to amphetamine and morphine

We next investigated acute psychomotor responses to the administration of either amphetamine (2.5 mg/kg, i.p.) or morphine (10 mg/kg, i.p.).

The locomotor response to amphetamine was similar in male and female *Gng7*$^{fl/fl}$D$_1$Cre$^+$ mice and WT littermates (males: main effect of "treatment" $F_{(1,14)} = 221.7$, $p < 0.001$, "genotype × treatment" interaction $F_{(1,14)} = 0.14$, NS; females: main effect of "treatment" $F_{(1,12)} = 232.9$, $p < 0.001$, "genotype × treatment" interaction $F_{(1,12)} = 0.24$, NS; Fig. 8*A*). In contrast, the locomotor response to amphetamine was markedly increased in male and female *Gng7*$^{fl/fl}$D$_2$Cre$^+$ mice compared with WT controls (Fig. 8*B*). Two-way ANOVA revealed a significant "genotype × treatment" interaction (males: $F_{(1,13)} = 7.6$, $p < 0.05$; females: $F_{(1,17)} = 8.0$, $p < 0.05$). *Post hoc* analysis confirmed that amphetamine-induced locomotion was enhanced in *Gng7*$^{fl/fl}$D$_2$Cre$^+$ mice of both sexes compared with *Gng7*$^{fl/fl}$ controls.

The locomotor response to morphine was markedly attenuated in male and female *Gng7*$^{fl/fl}$D$_1$Cre$^+$ mice compared with controls (Fig. 8*C*). Two-way ANOVA revealed a significant effect of "treatment" (males: $F_{(1,18)} = 82.4$, $p < 0.001$; females: $F_{(1,17)} = 19.2$, $p < 0.001$) and "genotype" (males: $F_{(1,18)} = 17.9$, $p < 0.001$; females: $F_{(1,17)} = 4.7$, $p < 0.05$), as well as a

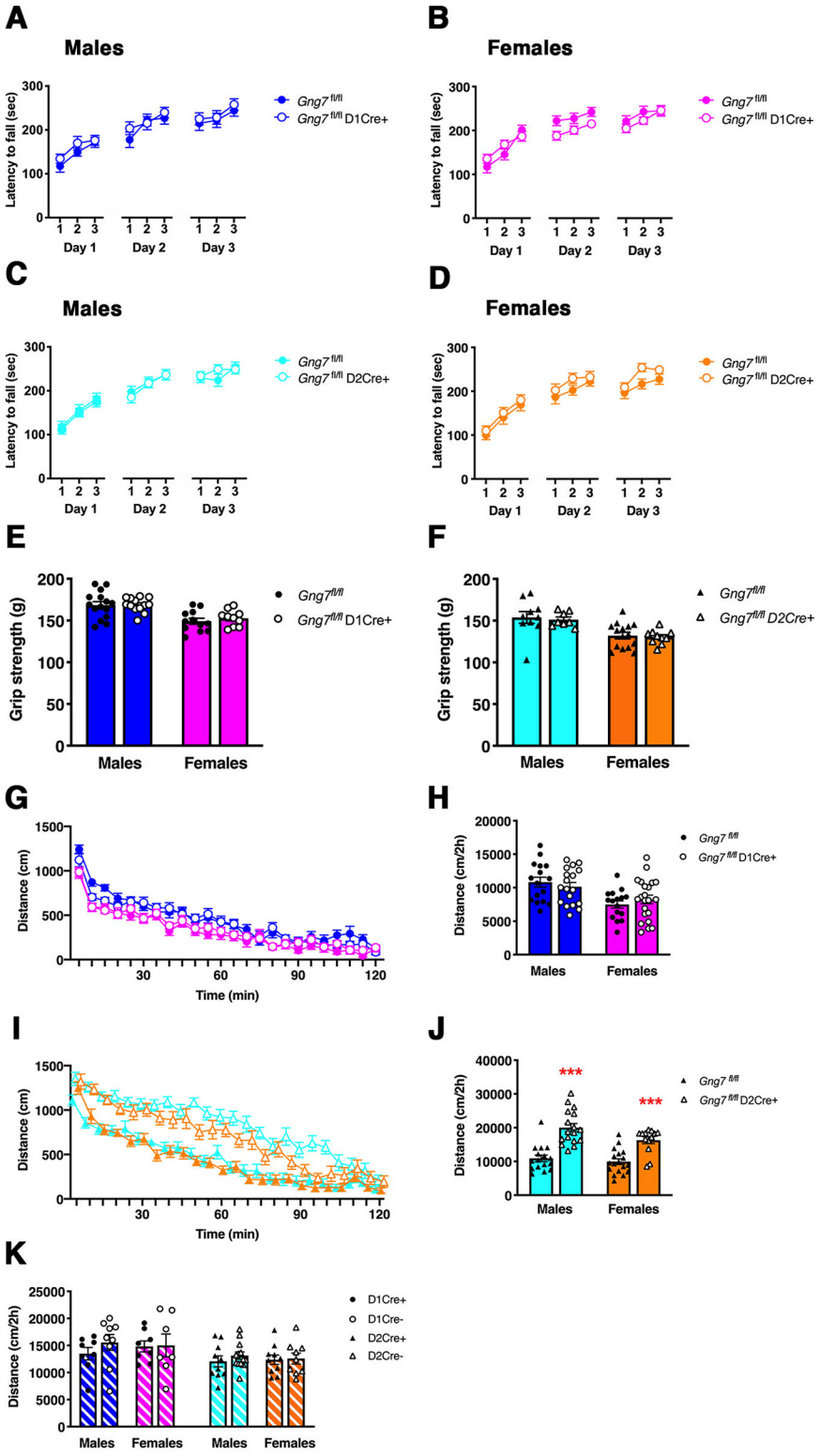

Figure 6. Assessment of motor coordination and muscular performance, as measured by the rotarod (***A–D***) and grip strength (***E,F***) tests and open field locomotor activity in conditional D_1R- and D_2R-γ_7 KO mice (***G–J***) or D_1R- and D_2R-Cre control mice (***K***). ***A–D***, Line graphs represent average latency to fall (seconds) in each trial over 3 d (9 trials/mouse) by male and female $Gng7^{fl/fl}D_1Cre^+$ (***A,B***), $Gng7^{fl/fl}D_2Cre^+$ mice (***C,D***), and relative littermate controls. Mice showed a progressive improvement in rotarod performance over multiple trials/days. Rotarod performance was comparable between male and females $Gng7^{fl/fl}D_1Cre^+$, $Gng7^{fl/fl}D_2Cre^+$ mice, and relative WT controls (three-way ANOVA and Tukey's *post hoc*, "trial × day × genotype" interaction: males $Gng7^{fl/fl}D_1Cre^+$ $F_{(4,124)} = 0.7$, NS; ***A***; females $Gng7^{fl/fl}D_1Cre^+$ $F_{(4,132)} = 1.5$, NS; ***B***; males $Gng7^{fl/fl}D_2Cre^+$ $F_{(4,148)} = 0.6$, NS; ***C***; females $Gng7^{fl/fl}D_1Cre^+$ $F_{(4,128)} = 0.26$, NS; ***D***). Data are mean ± SEM. $n = 17$-20 mice/group. ***E, F***, Bar graphs represent the average grip strength (maximum gram of force achieved by the forelimb during the test, average of 3 trials/mouse) of male and female D_1Cre^+ mice (***E***), D_2Cre^+ mice (***F***), and relative littermate controls. There was no genotype difference in the grip strength test (Student's *t* test). Data are mean ± SEM. $n = 8$-19 mice/group. ***G-J***, Line graphs represent tracks of distance traveled (centimeters) in 5 min bins over a 2 h testing period by male and female $Gng7^{fl/fl}D_1Cre^+$ (***G***), $Gng7^{fl/fl}D_2Cre^+$ mice (***I***), and relative littermate controls. Bar graphs represent cumulative distance traveled over the 2 h testing period by male and female $Gng7^{fl/fl}D_1Cre^+$ mice (***H***), $Gng7^{fl/fl}D_2Cre^+$ mice (***J***), and relative littermate controls. $Gng7^{fl/fl}D_2Cre^+$ mice showed a significant increase in locomotor activity; however, all groups acclimated to the open field arena and steadily reduced locomotor activity throughout the testing period. ***$p < 0.001$, significant difference between $Gng7^{fl/fl}D_2Cre^+$ and $Gng7^{fl/fl}$ WT littermates (Student's *t* test). Data are mean ± SEM. $n = 14$-21 mice/group. ***K***, Cumulative distance traveled over the 2 h testing period by male and female D_1Cre^+ and D_2Cre^+ mice and relative Cre^- littermate controls. No genotype differences were observed. Data are mean ± SEM. $n = 8$-13 mice/group.

significant "genotype × treatment" interaction (males: $F_{(1,18)} = 16.2$, $p < 0.001$; females: $F_{(1,17)} = 4.7$, $p < 0.05$). Tukey's *post hoc* analysis confirmed that locomotor response to morphine was significantly attenuated in $Gng7^{fl/fl}D_1Cre^+$ mice of both sexes. However, $Gng7^{fl/fl}D_2Cre^+$ mice showed unaltered locomotor response to morphine compared with WT littermates (males: main effect of "treatment" $F_{(1,17)} = 40.8$, $p < 0.001$, "genotype × treatment" interaction $F_{(1,17)} = 1.4$, NS; females: main effect of "treatment" $F_{(1,13)} = 37.7$, $p < 0.001$, "genotype × treatment" interaction $F_{(1,13)} = 0.6$, NS; Fig. 8*D*).

Together, these findings suggest that D_1R and A_{2A}R signaling via $G\alpha_{olf}\beta_2\gamma_7$ heterotrimer in distinct MSN populations is differentially involved in the psychomotor effects of amphetamine and morphine.

Amphetamine-induced phosphorylation of PKA substrates

Increased levels of cAMP resulting from D_1R stimulation by psychostimulants activate the cAMP-dependent protein kinases (PKA), which in turn increases the phosphorylation state of several targets including DARPP-32, ERK, rpS6, and GluR1 (Svenningsson et al., 2005; Valjent et al., 2005; Corvol et al., 2007; Biever et al., 2016). To further investigate the contribution of $G\alpha_{olf}\beta_2\gamma_7$/cAMP signal downstream D_1Rs and A_{2A}Rs, we measured the phosphorylation state of Ser845-GluR1, Thr202/Tyr204-ERK2, and Ser235/236-rpS6 in the striatal preparations from either $Gng7^{fl/fl}D_1Cre^+$ or $Gng7^{fl/fl}D_2Cre^+$ and their respective WT littermates, 20 min following a single injection of amphetamine (10 mg/kg, i.p.). Since we did not observe sex differences in locomotor responses to amphetamine (Fig. 8*A*),

Table 1. Open field activity of conditional D_1R- and D_2R-γ_7 KO mice and WT littermates[a]

	Males			Females		
	Vertical counts	Stereotypy	%Thigmotaxis	Vertical counts	Stereotypy	%Thigmotaxis
$Gng7^{fl/fl}$	1305 ± 125	18671 ± 1079	66.5 ± 1.2	1214 ± 124	14107 ± 900	71.4 ± 1.8
$Gng7^{fl/fl}D_1Cre^+$	1090 ± 92	18463 ± 799	67.6 ± 1.5	1127 ± 112	14387 ± 961	72.1 ± 2.1
$Gng7^{fl/fl}$	1080 ± 94	18893 ± 986	69.8 ± 1.2	1198 ± 100	15872 ± 888	72 ± 1.3
$Gng7^{fl/fl}D_2Cre^+$	1809 ± 122***	24966 ± 1227***	71.1 ± 1.1	1940 ± 233**	21084 ± 639***	74.1 ± 1.2

[a]Data are mean ± SEM; $n = 14$-21 mice/group. Average of cumulative vertical counts and stereotypic counts and % thigmotaxis (100* $\Sigma_{\text{distance periphery}}/\Sigma_{\text{tot distance}}$) over the 2 h testing period by male and female $Gng7^{fl/fl}D_1Cre^+$ mice, $Gng7^{fl/fl}D_2Cre^+$ mice, and relative littermate controls.
$^{**}p < 0.01$, $^{***}p < 0.001$, indicate significant difference between $Gng7^{fl/fl}D_2Cre^+$ mice and relative $Gng7^{fl/fl}$ WT littermates (Student's t test).

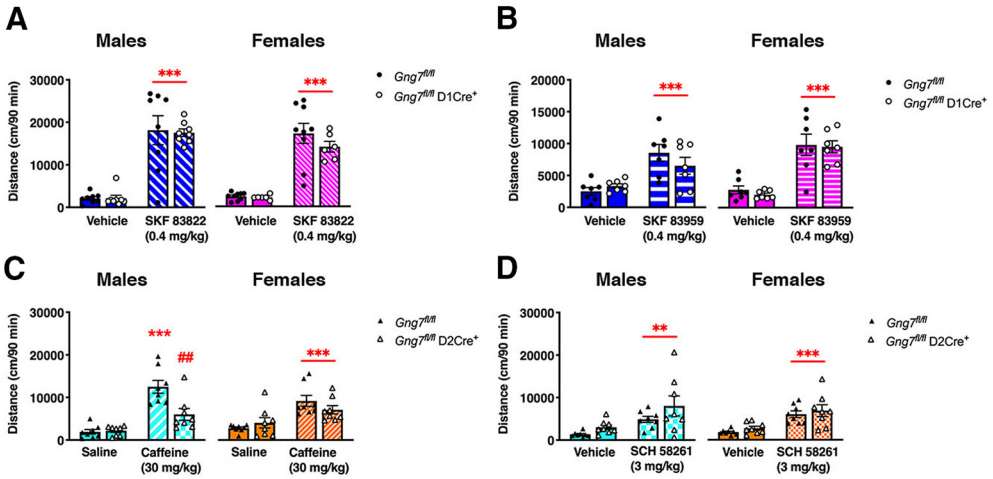

Figure 7. Acute locomotor activity in response to selective D_1R agonists and A_2AR antagonists. Mice were acclimated to the open field for 2 h on day 1. On day 2, mice were administered drug vehicle or saline 30 min after exposure to the open field and locomotor activity was monitored for additional 90 min. After 30 min acclimation on day 3, $Gng7^{fl/fl}D_1Cre^+$ mice and WT littermates were treated with D_1R agonists SKF 83822 (***A***) or SKF 83959 (***B***), while $Gng7^{fl/fl}D_2Cre^+$ mice and WT littermates were treated with A2AR antagonists caffeine (***C***) or SCH 58261 (***D***). The acute locomotor effect of drugs was evaluated over the following 90 min and compared with vehicle response on day 2. Male and female $Gng7^{fl/fl}D_1Cre^+$ and WT $Gng7^{fl/fl}$ mice showed equal locomotor response to both D_1R agonists (two-way repeated-measures ANOVA and Tukey's *post hoc*, $^{***}p < 0.001$, SKF 83822 or SKF 83959 vs vehicle). Male $Gng7^{fl/fl}D_2Cre^+$ mice showed an attenuated response to caffeine compared with $Gng7^{fl/fl}$ controls, while locomotor response to SCH 58261 did not differ between genotypes (two-way repeated-measures ANOVA and Tukey's *post hoc*, $^{***}p < 0.001$, $Gng7^{fl/fl}$ saline vs $Gng7^{fl/fl}$ caffeine; $^{\#\#}p < 0.01$, $Gng7^{fl/fl}$ caffeine vs $Gng7^{fl/fl}D_2Cre^+$ caffeine; $^{**}p < 0.01$, SCH 58261 vs vehicle). Female $Gng7^{fl/fl}D_2Cre^+$ and WT $Gng7^{fl/fl}$ mice showed equal locomotor response to both caffeine and SCH 58261 (two-way repeated-measures ANOVA and Tukey's *post hoc*, $^{***}p < 0.001$, caffeine or SCH 58261 vs saline or vehicle). Data are mean ± SEM. $n = 6$-9 mice/group.

balanced groups including both male and female mice were used for analysis. As expected, amphetamine treatment caused a marked increase in the phosphorylation states of all the proteins analyzed, with no effect on total levels of protein (Fig. 9*A*–*C*). Consistent with the lack of changes in amphetamine-induced locomotion, there was no observable reduction in Ser845-GluR1, Thr202/Tyr204-ERK2, and Ser235/236-rpS6 phosphorylation following amphetamine treatment in $Gng7^{fl/fl}D_1Cre^+$ mice compared with controls (p-GluR1: main effect of "treatment" $F_{(1,20)} = 73.3$, $p < 0.001$, "genotype × treatment" interaction $F_{(1,20)} = 3.2$, NS; p-ERK: main effect of "treatment" $F_{(1,20)} = 36.2$, $p < 0.001$, "genotype × treatment" interaction $F_{(1,20)} = 0.2$, NS; p-rpS6: main effect of "treatment" $F_{(1,20)} = 50$, $p < 0.001$, "genotype × treatment" interaction $F_{(1,20)} = 2.5$, NS; Fig. 9*A*–*C*).

Likewise, there was no difference in amphetamine-induced Ser845-GluR1, Thr202/Tyr204-ERK2, and Ser235/236-rpS6 phosphorylation in the striatum of $Gng7^{fl/fl}D_2Cre^+$ mice compared with WT littermates (p-GluR1: main effect of "treatment" $F_{(1,26)} = 20.4$, $p < 0.001$, "genotype × treatment" interaction $F_{(1,26)} = 0.05$, NS; p-ERK: main effect of "treatment" $F_{(1,26)} = 64.7$, $p < 0.001$, "genotype × treatment" interaction $F_{(1,26)} = 0.04$, NS; p-rpS6: main effect of "treatment" $F_{(1,26)} = 23.9$, $p < 0.001$, "genotype × treatment" interaction $F_{(1,26)} = 0.6$, NS; Fig. 9*D*–*F*). These results suggest that the lack of $G\alpha_{olf}\beta_2\gamma_7$ heterotrimer in either D_1R- and D_2R-MSNs does not affect amphetamine-induced phosphorylation of GluR1, ERK, and rpS6.

Increased cholinergic tone in the striatum reverses amphetamine-induced phosphorylation of PKA substrates

Several studies have demonstrated that acetylcholine release from cholinergic interneurons exerts a negative control on the integration of dopamine signals in D_1R-MSNs and affects dopamine-dependent behavior (Jeon et al., 2010; Kharkwal et al., 2016b; Nair et al., 2019). To test whether increased cholinergic neurotransmission affects amphetamine-induced phosphorylation of PKA substrates, we pretreated $Gng7^{fl/fl}D_1Cre^+$ and control mice with the acetylcholinesterase inhibitor donepezil 10 min before amphetamine. Three-way ANOVA confirmed the ability of amphetamine to increase the phosphorylation state of Ser845-GluR1, Thr202/Tyr204-ERK2, and Ser235/236-rpS6 in striatal preparations, independently of genotype (p-GluR1: main effect of "treatment" $F_{(1,53)} = 32.8$, $p < 0.001$, "genotype × treatment" interaction $F_{(1,53)} = 0.2$, NS; p-ERK: main effect of "treatment" $F_{(1,53)} = 26.8$, $p < 0.001$, "genotype × treatment" interaction $F_{(1,53)} = 0.005$, NS, p-rpS6: main effect of "treatment" $F_{(1,53)} = 25.7$, $p < 0.001$, "genotype × treatment" interaction $F_{(1,53)} = 2.6$, NS; Fig. 10*A*–*C*). Notably, pretreatment with donepezil did not affect baseline phosphorylation levels of

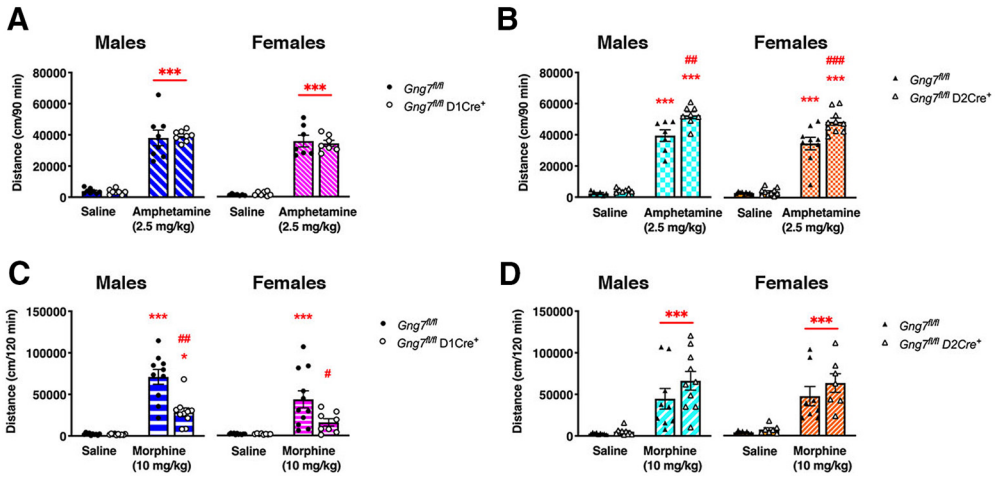

Figure 8. Acute locomotor activity in response to amphetamine and morphine. The acute locomotor effect of drugs was evaluated over 90 (amphetamine) or 120 (morphine) min following drug administration and compared with saline response on the previous day. Male and female *Gng7*$^{fl/fl}$D$_1$Cre$^+$ and WT *Gng7*$^{fl/fl}$ mice showed equal locomotor response to amphetamine (two-way repeated-measures ANOVA and Tukey's *post hoc*, $^{***}p < 0.001$ amphetamine vs saline, ***A***). In contrast, *Gng7*$^{fl/fl}$D$_2$Cre$^+$ mice showed an enhanced response to amphetamine compared with *Gng7*$^{fl/fl}$ controls (two-way repeated-measures ANOVA and Tukey's *post hoc*, $^{***}p < 0.01$ amphetamine vs saline; $^{\#\#}p < 0.01$, $^{\#\#\#}p < 0.001$, *Gng7*$^{fl/fl}$D$_2$Cre$^+$ amphetamine vs *Gng7*$^{fl/fl}$ amphetamine, ***B***). Morphine response was significantly attenuated in *Gng7*$^{fl/fl}$D$_1$Cre$^+$ mice (two-way repeated-measures ANOVA and Tukey's *post hoc*, $^{*}p < 0.05$, Gng7$^{fl/fl}$D$_1$Cre$^+$ morphine vs saline; $^{***}p < 0.001$, *Gng7*$^{fl/fl}$ morphine vs saline; $^{\#}p < 0.05$, $^{\#\#}p < 0.01$, *Gng7*$^{fl/fl}$D$_1$Cre$^+$ morphine vs *Gng7*$^{fl/fl}$ morphine; ***C***), while locomotor response to morphine of *Gng7*$^{fl/fl}$D$_2$Cre$^+$ mice was similar to controls (two-way repeated-measures ANOVA and Tukey's *post hoc*, $^{***}p < 0.001$ morphine vs saline, ***D***). Data are mean ± SEM. $n = 7$-11 mice/group.

Ser845-GluR1 and Ser235/236-rpS6, but reversed the amphetamine-induced phosphorylation of both proteins (p-GluR1: "pretreatment × treatment" interaction $F_{(1,53)} = 6.3$, $p < 0.05$; p-rpS6: "pretreatment × treatment" interaction $F_{(1,53)} = 6.2$, $p < 0.05$; Fig. 10*A*,*B*). Pretreatment with donepezil significantly reduced Thr202/Tyr204-ERK2 phosphorylation both at baseline and after amphetamine treatment (p-ERK: "pretreatment" effect $F_{(1,53)} = 10.9$, $p < 0.001$, "pretreatment × treatment" interaction $F_{(1,53)} = 1.1$, NS; Fig. 10*C*). None of the treatments affected total levels of GluR1, ERK, and rpS6. These findings suggest that increased cholinergic signaling alters phosphorylation of Ser845-GluR1 and Ser235/236-rpS6 induced by amphetamine.

Discussion

In this study, we leveraged conditional genetic mouse models to dissect the functions of a highly specialized G-protein heterotrimer composed of Gα_{olf}, β_2, and γ_7 subunits, that represents the main stimulatory pathway for cAMP production downstream D$_1$Rs and A$_{2A}$Rs in two distinct MSN populations. Consistent with our previous studies in global γ7 KO mice (Schwindinger et al., 2003, 2010), we show that targeted deletion of the γ_7 subunit in D$_1$R- or D$_2$R/A$_{2A}$R-MSNs leads to coordinated and cell type-specific suppression of Gα_{olf} protein levels, as well as selective defects in either D$_1$R- or A$_{2A}$R-stimulated cAMP production, respectively, without causing compensatory changes in other α and γ subunits.

Contrary to existing dogma (Xu et al., 1994; Herve et al., 2001; Bateup et al., 2010), we demonstrate that striatal D$_1$R signaling via G$\alpha_{olf}\beta_2\gamma_7$/cAMP pathway is not required for motor coordination, spontaneous locomotion, or psychomotor responses to D$_1$R-directed agonists and amphetamine. This is consistent with previous studies showing that selective enhancement of Gα_i- or Gα_s-mediated signaling in D$_1$R-MSNs of the dorsolateral striatum through viral-mediated DREADD expression does not impact locomotor behavior or acute responses to psychostimulants, but it is important in the regulation of behavioral adaptation because of repeated drug use and decision-making strategies during reward-based discrimination tasks (Ferguson et al., 2011, 2013). Furthermore, elimination of AC5 in mice, which leads to a severe impairment of striatal D$_1$R- and A$_{2A}$R-mediated cAMP production, is associated with deficits in striatum-dependent appetitive learning (Kheirbek et al., 2008, 2010), without altering psychomotor responses to the administration of D$_1$R agonists (Lee et al., 2002). Thus, it is possible that D$_1$R engage extrastriatal areas (Yano et al., 2018) and/or non–AC-dependent signaling pathways, such as phospholipase C and β-arrestin (Kuroiwa et al., 2008; Medvedev et al., 2013), to alter locomotor behavior.

Despite the clear reduction in Gα_{olf} expression relative to WTs in our *Gng7*$^{fl/fl}$D$_1$Cre$^+$ mouse model, amphetamine-induced phosphorylation of PKA substrates was preserved in these mice, which strengthens our behavioral data. This is surprising, given previous compelling evidence in *Gnal*$^{+/-}$ mice that acute locomotor and biochemical responses to psychostimulants are highly dependent on D$_1$R-Gα_{olf} signaling (Zhuang et al., 2000; Corvol et al., 2007; Alcacer et al., 2012; Biever et al., 2016).

The phenotypic differences between the *Gnal* and the *Gng7* KO mouse models may have multiple possible interpretations. First, residual cAMP production in D$_1$R-MSNs may result from an alternative heterotrimeric complex of Gα_{olf} with a γ subunit other than γ_7. Consistently, global *Gng7* gene deletion does not completely suppress Gα_{olf} protein levels (Schwindinger et al., 2003). Second, the deletion of Gα_{olf} signaling in both MSN populations of *Gnal* KO mice may have more profound consequences on psychostimulant-induced PKA activation compared with the selective disruption of Gα_{olf} signaling in discrete populations of MSNs described in this study. Indeed, PKA activity in D$_1$R-MSNs depends on psychostimulant action on both MSN subtypes, by modulation of their collateral interactions (Dobbs et al., 2016; Kharkwal et al., 2016a). Third, cholinergic interneuron control of striatal dopamine signal could play a role (Jeon et al., 2010; Kharkwal et al., 2016b; Nair et al., 2019). Gα_{olf} is expressed in striatal cholinergic interneurons (Herve et al., 2001), whereas Gα_{olf} haploinsufficiency leads to paradoxical enhanced cholinergic tone following dopaminergic stimulation (Eskow Jaunarajs et

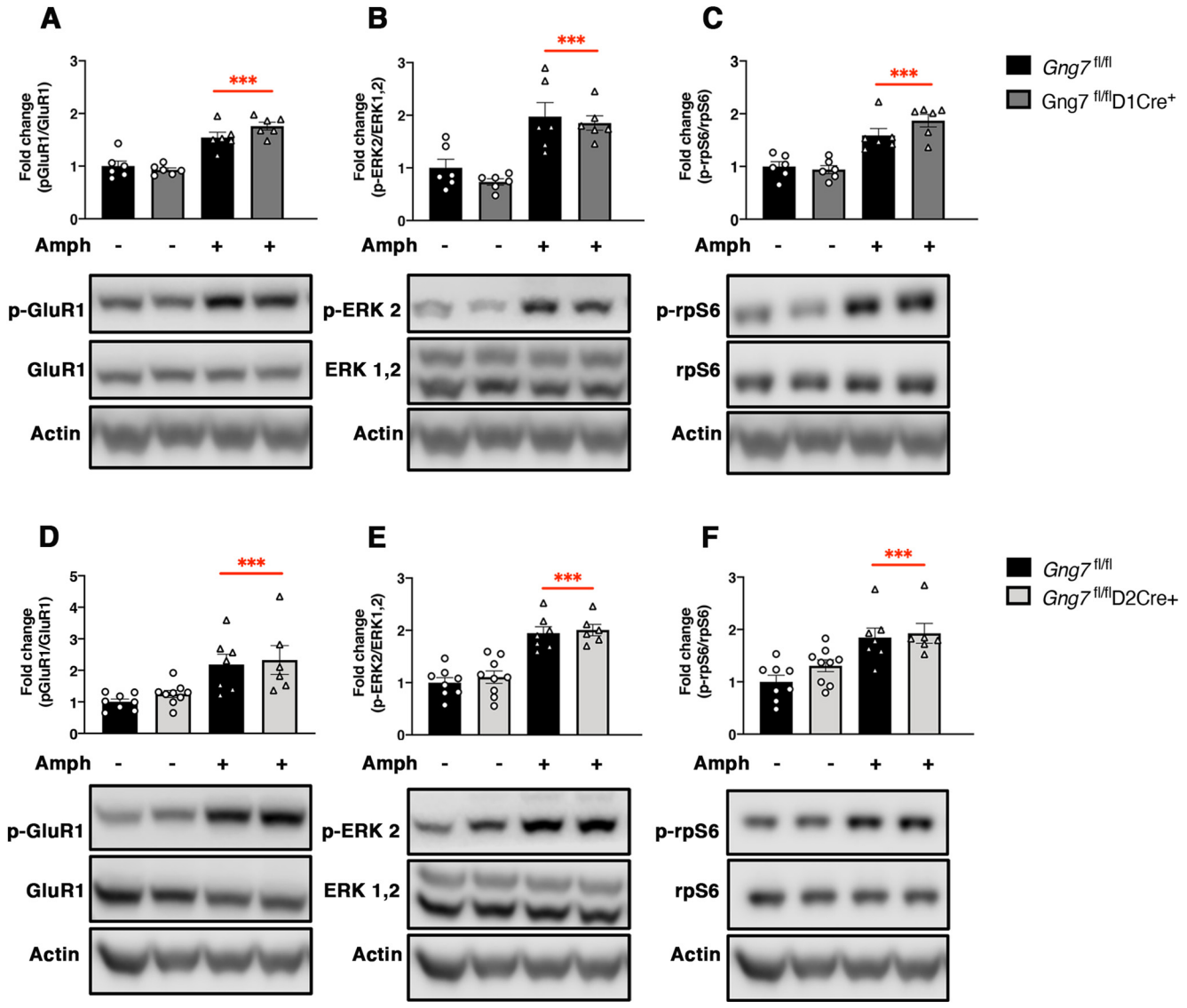

Figure 9. Amphetamine-induced phosphorylation of GluR1-Ser845, ERK2-Thr202/Tyr204, and rpS6-Ser235/23 in the striatum of conditional D_1R- and D_2R-γ_7 KO mice and WT littermates. Representative immunoblots and densitometric analysis of phosphorylated and total protein levels in striatal homogenates of $Gng7^{fl/fl}D_1Cre^+$ (***A–C***), $Gng7^{fl/fl}D_2Cre^+$ (***D-F***), and respective $Gng7^{fl/fl}$ WT mice, 20 min after injection of amphetamine (10 mg/kg) or saline. Each column represents a normalized ratio (fold-change) relative to total protein and to controls ($Gng7^{fl/fl}$ saline). The relative levels of GluR1, ERK1/2, and rpS6 were normalized to β-actin. Samples derive from the same experiment and the blots were processed in parallel. A loading control was included in each gel and was used to normalize data across multiple blots. Amphetamine-induced GluR1-Ser845, ERK1/2-Thr202/Tyr204, and rpS6-Ser235/23 phosphorylation was not significantly different in the striatum of $Gng7^{fl/fl}D_1Cre^+$ or $Gng7^{fl/fl}D_2Cre^+$ compared with $Gng7^{fl/fl}$ controls (two-way ANOVA and Tukey's *post hoc*: "main effect of treatment," $^{***}p < 0.001$ amphetamine vs saline). Total levels of GluR1, ERK, and rpS6 proteins were not affected by amphetamine. Data are mean ± SEM. $n = 6$-9 mice/group.

al., 2019) and altered pharmacological responses to cholinergic agents (Pelosi et al., 2017). In contrast, our ISH results show a few large-sized neurons expressing D_2Rs, presumably cholinergic interneurons, devoid of *Gng7* mRNA transcripts, which confirm our previous observation of low Gγ_7 levels in this neuronal population (Schwindinger et al., 2012). This suggests that loss of Gγ_7 subunit causes a selective reduction of Gα_{olf} signaling in MSNs while preserving its expression and function in cholinergic interneurons. We show here that enhanced cholinergic tone, induced by the acetylcholinesterase inhibitor donepezil, counteracts the effect of amphetamine on the phosphorylation of PKA substrates, including p-Ser845-GluR1 and p-Ser235/236-rpS6. This effect was comparable between $Gng7^{fl/fl}D_1Cre^+$ and WT mice and seems to parallel the reduced amphetamine-induced phosphorylation of p-Ser845-GluR1 and p-Ser235/236-rpS6 observed in $Gnal^{+/-}$ mice (Corvol et al., 2007; Biever et al., 2016). Thus, we suggest that dysfunctions of cholinergic interneurons, as described in the $Gnal^{+/-}$ mouse model, may have profound consequences on MSN activity, leading to less efficient activation of D_1R- and cAMP-dependent phosphorylation of PKA substrates.

We demonstrate that elimination of G$\alpha_{olf}\beta_2\gamma_7$ heterotrimer signal downstream of A_{2A}Rs in D_2R-MSNs results in a hyperlocomotor phenotype and increased sensitivity to the locomotor-enhancing effect of amphetamine. The hyperactivity observed in $Gng7^{fl/fl}D_2Cre^+$ mice seems to align with previous studies showing that D_2R-MSN ablation or D_2R-MSN-selective deletion of DARPP-32 or ERK causes an increase in spontaneous locomotor behavior in mice (Durieux et al., 2009; Bateup et al., 2010; Hutton et al., 2017) and points to a specific role of the G$\alpha_{olf}\beta_2\gamma_7$/cAMP signaling in the striatopallidal pathway for proper regulation of locomotor function. It is thought that tonic

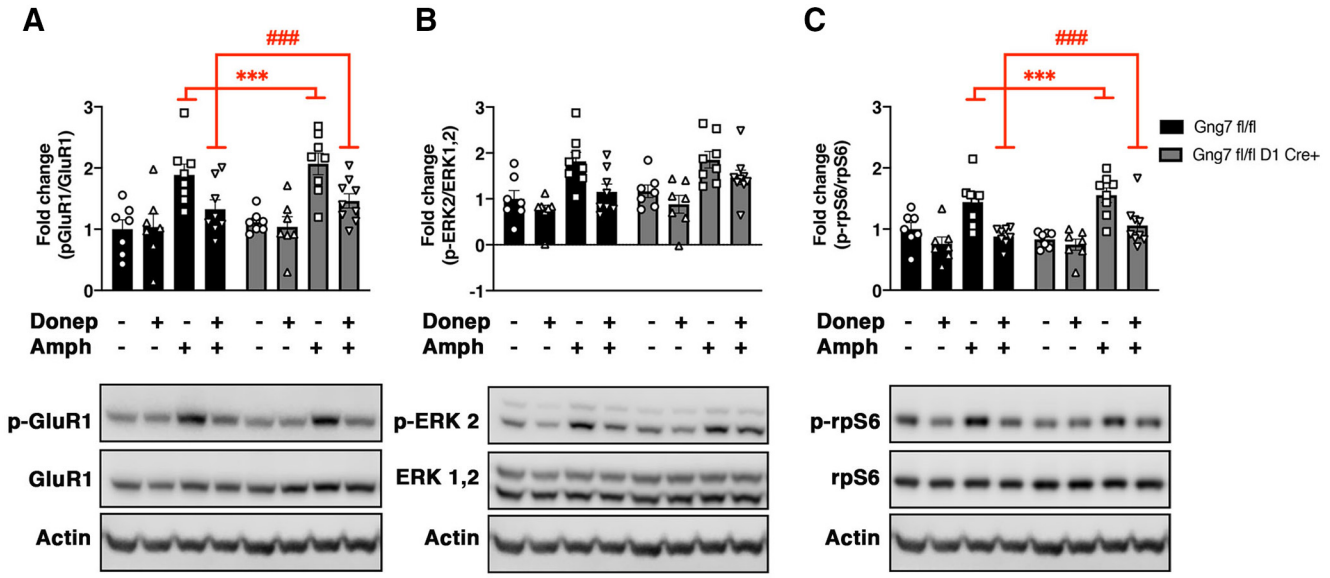

Figure 10. Reversal of amphetamine-induced phosphorylation of GluR1-Ser845, ERK1/2-Thr202/Tyr204, and rpS6-Ser235/23 by donepezil in the striatum of conditional D_1R-γ_7 KO mice and WT littermates. Representative immunoblots and densitometric analysis of phosphorylated and total protein levels in striatal homogenates of *Gng7*$^{fl/fl}D_1Cre^+$ and respective *Gng7*$^{fl/fl}$ WT mice. Mice were pretreated with donepezil (3 mg/kg) or saline 10 min before receiving an injection of amphetamine (10 mg/kg) or saline. Striatal tissues were collected 20 min after the amphetamine injection. Each column represents a normalized ratio (fold-change) relative to total protein and to controls (*Gng7*$^{fl/fl}$ saline). The relative levels of GluR1, ERK1/2, and rpS6 were normalized to β-actin. Samples derive from the same experiment and the blots were processed in parallel. A loading control was included in each gel and was used to normalize data across multiple blots. Amphetamine increased the phosphorylation state of GluR1-Ser845, ERK2-Thr202/Tyr204, and rpS6-Ser235/23 independently of genotype. Donepezil pretreatment significantly reduced the amphetamine-induced phosphorylation of GluR1-Ser845 (***A***) and rpS6-Ser235/23 (***C***) in both *Gng7*$^{fl/fl}D_1Cre^+$ and *Gng7*$^{fl/fl}$ WT mice (three-way ANOVA and Tukey's *post hoc*: "pretreatment × treatment" interaction, $^{***}p < 0.001$ saline-amphetamine vs saline-saline; $^{###}p < 0.001$ donepezil-amphetamine vs saline-amphetamine). Donepezil pretreatment reduced ERK2-Thr202/Tyr204 phosphorylation (***B***) both at baseline and after amphetamine treatment. Total levels of GluR1, ERK, and rpS6 proteins were not affected by amphetamine or donepezil treatment. Data are mean ± SEM. $n = 7$-9 mice/group.

dopamine release enables motor functions through preferential activation of high-affinity D_2Rs (Richfield et al., 1989; Grace et al., 2007), while phasic bursts of dopamine firing associated with reward signals or stimulated by drugs of abuse are partially mediated by D_2Rs and preferentially activate D_1Rs (Hikida et al., 2010; Marcott et al., 2014). Additionally, several studies have shown that $A_{2A}R$-$G\alpha_{olf}$ signal in D_2R-MSNs profoundly influences dopaminergic actions through antagonistic interaction with D_2Rs-$G\alpha_{i/o}$ at the AC level (Svenningsson et al., 2000; Shen and Chen, 2009; Ferré et al., 2018). For example, activation of $A_{2A}Rs$ blocks D_2R-mediated behavioral and biochemical responses and inhibits amphetamine-induced locomotion in mice (Turgeon et al., 1996; Rimondini et al., 1997; Hakansson et al., 2006), whereas $A_{2A}Rs$ antagonists potentiate the acute motor effects amphetamine and L-DOPA (Fenu et al., 1997; Poleszak and Malec, 2000). Based on the collective evidence, it is our hypothesis that selective loss of $A_{2A}R$-$G\alpha_{olf}$ signaling pathway in D_2R-MSNs relieves inhibition of D_2R-$G_{i/o}$ signaling, resulting in hyperlocomotion and enhanced responsiveness to the effects of amphetamine in *Gng7*$^{fl/fl}D_2Cre^+$ mice. However, since significant *Gng7* recombination was observed in the midbrain of *Gng7*$^{fl/fl}D_2Cre^+$ mice, we cannot rule out the possibility that recombination of *Gng7* in D2R-expressing dopamine neurons causes changes in dopamine neurotransmission, thus contributing to the locomotor effects observed in these mice. Future studies will address the consequences of $A_{2A}R$-G_{olf} signal loss on striatal D_2Rs expression and function, as well as changes in dopamine neurotransmission in *Gng7*$^{fl/fl}D_2Cre^+$ mice.

In this study, we show a specific requirement for $G\alpha_{olf}\beta_2\gamma_7$ signaling acting downstream of D_1Rs to mediate the acute locomotor-enhancing properties of morphine. Increased dopaminergic transmission in the striatum is considered a common step through which addictive drugs, including morphine, exert locomotor-enhancing and rewarding effects in rodents (Di Chiara and Imperato, 1988; Spanagel et al., 1990; Johnson and North, 1992). However, locomotor and rewarding responses to opioids can also be induced via direct actions on MORs in striatal neurons (Stevens et al., 1986; Vaccarino et al., 1986; Cui et al., 2014). Several lines of evidence also suggest a role for striatal D_1R-dependent signaling for a multifaceted mediation of morphine locomotor behavior (Borgkvist et al., 2007; Urs et al., 2011; Tao et al., 2017). One point of convergence between MOR and D_1R signals is represented by MSNs residing in the striosome compartment (Miura et al., 2008; Crittenden et al., 2016). Additionally, both MORs and D_1Rs show a requirement for AC5 to oppositely regulate cAMP production in the striatum. Similar to our results, lack of AC5 in mice results in loss of locomotor responses by morphine (Kim et al., 2006), while locomotion following D_1R agonists administration is preserved (Lee et al., 2002). Here, we showed that D_1R-MSN specific deletion of γ_7 affects the distributional pattern of $G\alpha_{olf}$ expression in the striosome and matrix compartment, as evidenced by a significant reduction of $G\alpha_{olf}$ immunoreactivity in the MOR-enriched striosomes of *Gng7*$^{fl/fl}D_1Cre^+$ mice. Furthermore, we detected a small (~20%) but significant decrease in AC5 expression in striatal membranes of *Gng7*$^{fl/fl}D_1Cre^+$ mice. Therefore, it is possible that the loss of AC5 protein in D_1R-MSNs, likely in the striosome compartment, accounts for the reduction of locomotor response to morphine observed in *Gng7*$^{fl/fl}D_1Cre^+$ mice. On the other hand, we can exclude a contribution of $G\alpha_{olf}$/cAMP signaling in D_2R-MSNs, since morphine equally enhanced locomotor activity in *Gng7*$^{fl/fl}D_2Cre^+$ mice and WT littermates. Although further work is needed to address the interactions between opioid and dopamine receptor systems in the striatum, our

results establish additional evidence for a role of cAMP signal in D_1R-MSNs for morphine-induced locomotion.

In conclusion, our results revealed that striatal cAMP signaling mediated by the $G\alpha_{olf}\beta_2\gamma_7$ heterotrimer in discrete MSN populations differentially regulates motor behavior in mice. We demonstrate that the $G\alpha_{olf}\beta_2\gamma_7$ heterotrimer is not key to activation of PKA signaling by amphetamine. We also demonstrate that amphetamine-induced PKA activity can be finely modulated by release of striatal acetylcholine. Our results do not exclude the possibility that other cAMP effectors, such as the guanine nucleotide exchange factor EPAC (Robichaux and Cheng, 2018) as well as $G\beta\gamma$-regulated effectors (Khan et al., 2013; Smrcka and Fisher, 2019), could contribute to the behavioral phenotype observed in our mouse model. Nevertheless, the identification of γ_7 as central regulator of striatal cAMP signaling pathways paves the way to further avenues for investigation and therapeutic options for conditions, such as Parkinson's disease, dystonia, drug addiction, and schizophrenia, where these pathways are dysfunctional.

References

Abudukeyoumu N, Hernandez-Flores T, Garcia-Munoz M, Arbuthnott GW (2019) Cholinergic modulation of striatal microcircuits. Eur J Neurosci 49:604–622.

Albin RL, Young AB, Penney JB (1989) The functional anatomy of basal ganglia disorders. Trends Neurosci 12:366–375.

Alcacer C, Santini E, Valjent E, Gaven F, Girault JA, Herve D (2012) Galpha (olf) mutation allows parsing the role of cAMP-dependent and extracellular signal-regulated kinase-dependent signaling in L-3,4-dihydroxyphenylalanine-induced dyskinesia. J Neurosci 32:5900–5910.

Bateup HS, Santini E, Shen W, Birnbaum S, Valjent E, Surmeier DJ, Fisone G, Nestler EJ, Greengard P (2010) Distinct subclasses of medium spiny neurons differentially regulate striatal motor behaviors. Proc Natl Acad Sci USA 107:14845–14850.

Belluscio L, Gold GH, Nemes A, Axel R (1998) Mice deficient in G(olf) are anosmic. Neuron 20:69–81.

Biever A, Boubaker-Vitre J, Cutando L, Gracia-Rubio I, Costa-Mattioli M, Puighermanal E, Valjent E (2016) Repeated exposure to D-amphetamine decreases global protein synthesis and regulates the translation of a subset of mRNAs in the striatum. Front Mol Neurosci 9:165.

Borgkvist A, Usiello A, Greengard P, Fisone G (2007) Activation of the cAMP/PKA/DARPP-32 signaling pathway is required for morphine psychomotor stimulation but not for morphine reward. Neuropsychopharmacology 32:1995–2003.

Bychkov E, Zurkovsky L, Garret MB, Ahmed MR, Gurevich EV (2012) Distinct cellular and subcellular distributions of G protein-coupled receptor kinase and arrestin isoforms in the striatum. PLoS One 7:e48912.

Corvol JC, Studler JM, Schonn JS, Girault JA, Herve D (2001) Galpha(olf) is necessary for coupling D1 and A2a receptors to adenylyl cyclase in the striatum. J Neurochem 76:1585–1588.

Corvol JC, Valjent E, Pascoli V, Robin A, Stipanovich A, Luedtke RR, Belluscio L, Girault JA, Herve D (2007) Quantitative changes in Galphaolf protein levels, but not D1 receptor, alter specifically acute responses to psychostimulants. Neuropsychopharmacology 32:1109–1121.

Crittenden JR, Tillberg PW, Riad MH, Shima Y, Gerfen CR, Curry J, Housman DE, Nelson SB, Boyden ES, Graybiel AM (2016) Striosome-dendron bouquets highlight a unique striatonigral circuit targeting dopamine-containing neurons. Proc Natl Acad Sci USA 113:11318–11323.

Cui Y, Ostlund SB, James AS, Park CS, Ge W, Roberts KW, Mittal N, Murphy NP, Cepeda C, Kieffer BL, Levine MS, Jentsch JD, Walwyn WM, Sun YE, Evans CJ, Maidment NT, Yang XW (2014) Targeted expression of mu-opioid receptors in a subset of striatal direct-pathway neurons restores opiate reward. Nat Neurosci 17:254–261.

Di Chiara G, Imperato A (1988) Drugs abused by humans preferentially increase synaptic dopamine concentrations in the mesolimbic system of freely moving rats. Proc Natl Acad Sci USA 85:5274–5278.

Dobbs LK, Kaplan AR, Lemos JC, Matsui A, Rubinstein M, Alvarez VA (2016) Dopamine regulation of lateral inhibition between striatal neurons gates the stimulant actions of cocaine. Neuron 90:1100–1113.

Durieux PF, Bearzatto B, Guiducci S, Buch T, Waisman A, Zoli M, Schiffmann SN, de Kerchove d'Exaerde A (2009) D2R striatopallidal neurons inhibit both locomotor and drug reward processes. Nat Neurosci 12:393–395.

Durieux PF, Schiffmann SN, de Kerchove d'Exaerde A (2012) Differential regulation of motor control and response to dopaminergic drugs by D1R and D2R neurons in distinct dorsal striatum subregions. EMBO J 31:640–653.

Eskow Jaunarajs KL, Scarduzio M, Ehrlich ME, McMahon LL, Standaert DG (2019) Diverse mechanisms lead to common dysfunction of striatal cholinergic interneurons in distinct genetic mouse models of dystonia. J Neurosci 39:7195–7205.

Farrell MS, Pei Y, Wan Y, Yadav PN, Daigle TL, Urban DJ, Lee HM, Sciaky N, Simmons A, Nonneman RJ, Huang XP, Hufeisen SJ, Guettier JM, Moy SS, Wess J, Caron MG, Calakos N, Roth BL (2013) A Galphas DREADD mouse for selective modulation of cAMP production in striatopallidal neurons. Neuropsychopharmacology 38:854–862.

Fenu S, Pinna A, Ongini E, Morelli M (1997) Adenosine A2A receptor antagonism potentiates L-DOPA-induced turning behaviour and c-fos expression in 6-hydroxydopamine-lesioned rats. Eur J Pharmacol 321:143–147.

Ferguson SM, Eskenazi D, Ishikawa M, Wanat MJ, Phillips PE, Dong Y, Roth BL, Neumaier JF (2011) Transient neuronal inhibition reveals opposing roles of indirect and direct pathways in sensitization. Nat Neurosci 14:22–24.

Ferguson SM, Phillips PE, Roth BL, Wess J, Neumaier JF (2013) Direct-pathway striatal neurons regulate the retention of decision-making strategies. J Neurosci 33:11668–11676.

Ferré S, Bonaventura J, Zhu W, Hatcher-Solis C, Taura J, Quiroz C, Cai NS, Moreno E, Casadó-Anguera V, Kravitz AV, Thompson KR, Tomasi DG, Navarro G, Cordomí A, Pardo L, Lluís C, Dessauer CW, Volkow ND, Casadó V, Ciruela F, et al. (2018) Essential control of the function of the striatopallidal neuron by pre-coupled complexes of adenosine A2A-dopamine D2 receptor heterotetramers and adenylyl cyclase. Front Pharmacol 9:243.

Fuchs T, Saunders-Pullman R, Masuho I, Luciano MS, Raymond D, Factor S, Lang AE, Liang TW, Trosch RM, White S, Ainehsazan E, Herve D, Sharma N, Ehrlich ME, Martemyanov KA, Bressman SB, Ozelius LJ (2013) Mutations in GNAL cause primary torsion dystonia. Nat Genet 45:88–92.

Gerfen CR, Engber TM, Mahan LC, Susel Z, Chase TN, Monsma FJ Jr, Sibley DR (1990) D1 and D2 dopamine receptor-regulated gene expression of striatonigral and striatopallidal neurons. Science 250:1429–1432.

Gerfen CR, Surmeier DJ (2011) Modulation of striatal projection systems by dopamine. Annu Rev Neurosci 34:441–466.

Gong S, Doughty M, Harbaugh CR, Cummins A, Hatten ME, Heintz N, Gerfen CR (2007) Targeting Cre recombinase to specific neuron populations with bacterial artificial chromosome constructs. J Neurosci 27:9817–9823.

Grace AA, Floresco SB, Goto Y, Lodge DJ (2007) Regulation of firing of dopaminergic neurons and control of goal-directed behaviors. Trends Neurosci 30:220–227.

Hakansson K, Galdi S, Hendrick J, Snyder G, Greengard P, Fisone G (2006) Regulation of phosphorylation of the GluR1 AMPA receptor by dopamine D2 receptors. J Neurochem 96:482–488.

Herve D, Le Moine C, Corvol JC, Belluscio L, Ledent C, Fienberg AA, Jaber M, Studler JM, Girault JA (2001) Galpha(olf) levels are regulated by receptor usage and control dopamine and adenosine action in the striatum. J Neurosci 21:4390–4399.

Hikida T, Kimura K, Wada N, Funabiki K, Nakanishi S (2010) Distinct roles of synaptic transmission in direct and indirect striatal pathways to reward and aversive behavior. Neuron 66:896–907.

Hutton SR, Otis JM, Kim EM, Lamsal Y, Stuber GD, Snider WD (2017) ERK/MAPK signaling is required for pathway-specific striatal motor functions. J Neurosci 37:8102–8115.

Iwamoto T, Iwatsubo K, Okumura S, Hashimoto Y, Tsunematsu T, Toya Y, Herve D, Umemura S, Ishikawa Y (2004) Disruption of type 5 adenylyl cyclase negates the developmental increase in Galphaolf expression in the striatum. FEBS Lett 564:153–156.

Jeon J, Dencker D, Wortwein G, Woldbye DP, Cui Y, Davis AA, Levey AI, Schutz G, Sager TN, Mork A, Li C, Deng CX, Fink-Jensen A, Wess J (2010) A subpopulation of neuronal M4 muscarinic acetylcholine receptors plays a critical role in modulating dopamine-dependent behaviors. J Neurosci 30:2396–2405.

Jin LQ, Goswami S, Cai G, Zhen X, Friedman E (2003) SKF83959 selectively regulates phosphatidylinositol-linked D1 dopamine receptors in rat brain. J Neurochem 85:378–386.

Johnson SW, North RA (1992) Opioids excite dopamine neurons by hyperpolarization of local interneurons. J Neurosci 12:483–488.

Jones DT, Reed RR (1989) Golf: an olfactory neuron specific-G protein involved in odorant signal transduction. Science 244:790–795.

Kerr DS, Von Dannecker LE, Davalos M, Michaloski JS, Malnic B (2008) Ric-8B interacts with G alpha olf and G gamma 13 and co-localizes with G alpha olf, G beta 1 and G gamma 13 in the cilia of olfactory sensory neurons. Mol Cell Neurosci 38:341–348.

Khan SM, Sleno R, Gora S, Zylbergold P, Laverdure JP, Labbe JC, Miller GJ, Hebert TE (2013) The expanding roles of Gbetagamma subunits in G protein-coupled receptor signaling and drug action. Pharmacol Rev 65:545–577.

Kharkwal G, Radl D, Lewis R, Borrelli E (2016a) Dopamine D2 receptors in striatal output neurons enable the psychomotor effects of cocaine. Proc Natl Acad Sci USA 113:11609–11614.

Kharkwal G, Brami-Cherrier K, Lizardi-Ortiz JE, Nelson AB, Ramos M, Del Barrio D, Sulzer D, Kreitzer AC, Borrelli E (2016b) Parkinsonism driven by antipsychotics originates from dopaminergic control of striatal cholinergic interneurons. Neuron 91:67–78.

Kheirbek MA, Beeler JA, Ishikawa Y, Zhuang X (2008) A cAMP pathway underlying reward prediction in associative learning. J Neurosci 28:11401–11408.

Kheirbek MA, Beeler JA, Chi W, Ishikawa Y, Zhuang X (2010) A molecular dissociation between cued and contextual appetitive learning. Learn Mem 17:148–154.

Kim KS, Lee KW, Lee KW, Im JY, Yoo JY, Kim SW, Lee JK, Nestler EJ, Han PL (2006) Adenylyl cyclase type 5 (AC5) is an essential mediator of morphine action. Proc Natl Acad Sci USA 103:3908–3913.

Kravitz AV, Freeze BS, Parker PR, Kay K, Thwin MT, Deisseroth K, Kreitzer AC (2010) Regulation of parkinsonian motor behaviours by optogenetic control of basal ganglia circuitry. Nature 466:622–626.

Kuroiwa M, Bateup HS, Shuto T, Higashi H, Tanaka M, Nishi A (2008) Regulation of DARPP-32 phosphorylation by three distinct dopamine D1-like receptor signaling pathways in the neostriatum. J Neurochem 107:1014–1026.

Lee KW, Hong JH, Choi IY, Che Y, Lee JK, Yang SD, Song CW, Kang HS, Lee JH, Noh JS, Shin HS, Han PL (2002) Impaired D2 dopamine receptor function in mice lacking type 5 adenylyl cyclase. J Neurosci 22:7931–7940.

Li F, Ponissery-Saidu S, Yee KK, Wang H, Chen ML, Iguchi N, Zhang G, Jiang P, Reisert J, Huang L (2013) Heterotrimeric G protein subunit Gγ13 is critical to olfaction. J Neurosci 33:7975–7984.

Lovinger DM (2010) Neurotransmitter roles in synaptic modulation, plasticity and learning in the dorsal striatum. Neuropharmacology 58:951–961.

Marcott PF, Mamaligas AA, Ford CP (2014) Phasic dopamine release drives rapid activation of striatal D2-receptors. Neuron 84:164–176.

Masuho I, Skamangas NK, Muntean BS, Martemyanov KA (2021) Diversity of the Gbetagamma complexes defines spatial and temporal bias of GPCR signaling. Cell Syst 12:324–337.e5.

Medvedev IO, Ramsey AJ, Masoud ST, Bermejo MK, Urs N, Sotnikova TD, Beaulieu JM, Gainetdinov RR, Salahpour A (2013) D1 dopamine receptor coupling to PLCbeta regulates forward locomotion in mice. J Neurosci 33:18125–18133.

Miura M, Masuda M, Aosaki T (2008) Roles of micro-opioid receptors in GABAergic synaptic transmission in the striosome and matrix compartments of the striatum. Mol Neurobiol 37:104–115.

Nair AG, Castro LR, El Khoury M, Gorgievski V, Giros B, Tzavara ET, Hellgren-Kotaleski J, Vincent P (2019) The high efficacy of muscarinic M4 receptor in D1 medium spiny neurons reverses striatal hyperdopaminergia. Neuropharmacology 146:74–83.

Nelson AB, Kreitzer AC (2014) Reassessing models of basal ganglia function and dysfunction. Annu Rev Neurosci 37:117–135.

Orru M, Bakesova J, Brugarolas M, Quiroz C, Beaumont V, Goldberg SR, Lluis C, Cortes A, Franco R, Casado V, Canela EI, Ferré S (2011) Striatal pre- and postsynaptic profile of adenosine A(2A) receptor antagonists. PLoS One 6:e16088.

O'Sullivan GJ, Dunleavy M, Hakansson K, Clementi M, Kinsella A, Croke DT, Drago J, Fienberg AA, Greengard P, Sibley DR, Fisone G, Henshall DC, Waddington JL (2008) Dopamine D1 vs D5 receptor-dependent induction of seizures in relation to DARPP-32, ERK1/2 and GluR1-AMPA signalling. Neuropharmacology 54:1051–1061.

Ozawa A, Brunori G, Mercatelli D, Wu J, Cippitelli A, Zou B, Xie XS, Williams M, Zaveri NT, Low S, Scherrer G, Kieffer BL, Toll L (2015) Knock-in mice with NOP-eGFP receptors identify receptor cellular and regional localization. J Neurosci 35:11682–11693.

Pelosi A, Menardy F, Popa D, Girault JA, Herve D (2017) Heterozygous Gnal mice are a novel animal model with which to study dystonia pathophysiology. J Neurosci 37:6253–6267.

Peterson SM, Pack TF, Wilkins AD, Urs NM, Urban DJ, Bass CE, Lichtarge O, Caron MG (2015) Elucidation of G-protein and beta-arrestin functional selectivity at the dopamine D2 receptor. Proc Natl Acad Sci USA 112:7097–7102.

Poleszak E, Malec D (2000) Influence of adenosine receptor agonists and antagonists on amphetamine-induced stereotypy in rats. Pol J Pharmacol 52:423–429.

Richfield EK, Penney JB, Young AB (1989) Anatomical and affinity state comparisons between dopamine D1 and D2 receptors in the rat central nervous system. Neuroscience 30:767–777.

Rimondini R, Ferré S, Ogren SO, Fuxe K (1997) Adenosine A2A agonists: a potential new type of atypical antipsychotic. Neuropsychopharmacology 17:82–91.

Robichaux WG 3rd, Cheng X (2018) Intracellular cAMP sensor EPAC: physiology, pathophysiology, and therapeutics development. Physiol Rev 98:919–1053.

Robishaw JD, Berlot CH (2004) Translating G protein subunit diversity into functional specificity. Curr Opin Cell Biol 16:206–209.

Rosenbaum DM, Rasmussen SG, Kobilka BK (2009) The structure and function of G-protein-coupled receptors. Nature 459:356–363.

Roth BL, Irwin JJ, Shoichet BK (2017) Discovery of new GPCR ligands to illuminate new biology. Nat Chem Biol 13:1143–1151.

Ruiz-DeDiego I, Naranjo JR, Hervé D, Moratalla R (2015) Dopaminergic regulation of olfactory type G-protein alpha subunit expression in the striatum. Mov Disord 30:1039–1049.

Sasaki K, Yamasaki T, Omotuyi IO, Mishina M, Ueda H (2013) Age-dependent dystonia in striatal Ggamma7 deficient mice is reversed by the dopamine D2 receptor agonist pramipexole. J Neurochem 124:844–854.

Schwindinger WF, Betz KS, Giger KE, Sabol A, Bronson SK, Robishaw JD (2003) Loss of G protein gamma 7 alters behavior and reduces striatal alpha(olf) level and cAMP production. J Biol Chem 278:6575–6579.

Schwindinger WF, Mihalcik LJ, Giger KE, Betz KS, Stauffer AM, Linden J, Herve D, Robishaw JD (2010) Adenosine A2A receptor signaling and golf assembly show a specific requirement for the gamma7 subtype in the striatum. J Biol Chem 285:29787–29796.

Schwindinger WF, Mirshahi UL, Baylor KA, Sheridan KM, Stauffer AM, Usefof S, Stecker MM, Mirshahi T, Robishaw JD (2012) Synergistic roles for G-protein gamma3 and gamma7 subtypes in seizure susceptibility as revealed in double knock-out mice. J Biol Chem 287:7121–7133.

Shen HY, Chen JF (2009) Adenosine A(2A) receptors in psychopharmacology: modulators of behavior, mood and cognition. Curr Neuropharmacol 7:195–206.

Smrcka AV, Fisher I (2019) G-protein betagamma subunits as multi-functional scaffolds and transducers in G-protein-coupled receptor signaling. Cell Mol Life Sci 76:4447–4459.

Spanagel R, Herz A, Shippenberg TS (1990) The effects of opioid peptides on dopamine release in the nucleus accumbens: an in vivo microdialysis study. J Neurochem 55:1734–1740.

Stevens KE, Mickley GA, McDermott LJ (1986) Brain areas involved in production of morphine-induced locomotor hyperactivity of the C57B1/6J mouse. Pharmacol Biochem Behav 24:1739–1747.

Svenningsson P, Lindskog M, Ledent C, Parmentier M, Greengard P, Fredholm BB, Fisone G (2000) Regulation of the phosphorylation of the dopamine- and cAMP-regulated phosphoprotein of 32 kDa in vivo by dopamine D1, dopamine D2, and adenosine A2A receptors. Proc Natl Acad Sci USA 97:1856–1860.

Svenningsson P, Nairn AC, Greengard P (2005) DARPP-32 mediates the actions of multiple drugs of abuse. AAPS J 7:E353–E360.

Tao YM, Yu C, Wang WS, Hou YY, Xu XJ, Chi ZQ, Ding YQ, Wang YJ, Liu JG (2017) Heteromers of mu opioid and dopamine D1 receptors modulate opioid-induced locomotor sensitization in a dopamine-independent manner. Br J Pharmacol 174:2842–2861.

Tepper JM, Koos T, Ibanez-Sandoval O, Tecuapetla F, Faust TW, Assous M (2018) Heterogeneity and diversity of striatal GABAergic interneurons: update 2018. Front Neuroanat 12:91.

Turgeon SM, Pollack AE, Schusheim L, Fink JS (1996) Effects of selective adenosine A1 and A2a agonists on amphetamine-induced locomotion and c-Fos in striatum and nucleus accumbens. Brain Res 707:75–80.

Undie AS, Weinstock J, Sarau HM, Friedman E (1994) Evidence for a distinct D1-like dopamine receptor that couples to activation of phosphoinositide metabolism in brain. J Neurochem 62:2045–2048.

Urs NM, Daigle TL, Caron MG (2011) A dopamine D1 receptor-dependent beta-arrestin signaling complex potentially regulates morphine-induced psychomotor activation but not reward in mice. Neuropsychopharmacology 36:551–558.

Vaccarino FJ, Amalric M, Swerdlow NR, Koob GF (1986) Blockade of amphetamine but not opiate-induced locomotion following antagonism of dopamine function in the rat. Pharmacol Biochem Behav 24:61–65.

Valjent E, Pascoli V, Svenningsson P, Paul S, Enslen H, Corvol JC, Stipanovich A, Caboche J, Lombroso PJ, Nairn AC, Greengard P, Herve D, Girault JA (2005) Regulation of a protein phosphatase cascade allows convergent dopamine and glutamate signals to activate ERK in the striatum. Proc Natl Acad Sci USA 102:491–496.

Watson JB, Coulter PM 2nd, Margulies JE, de Lecea L, Danielson PE, Erlander MG, Sutcliffe JG (1994) G-protein gamma 7 subunit is selectively expressed in medium-sized neurons and dendrites of the rat neostriatum. J Neurosci Res 39:108–116.

Xie K, Martemyanov KA (2011) Control of striatal signaling by g protein regulators. Front Neuroanat 5:49.

Xie K, Masuho I, Shih CC, Cao Y, Sasaki K, Lai CW, Han PL, Ueda H, Dessauer CW, Ehrlich ME, Xu B, Willardson BM, Martemyanov KA (2015) Stable G protein-effector complexes in striatal neurons: mechanism of assembly and role in neurotransmitter signaling. Elife 4: e10451.

Xu M, Hu XT, Cooper DC, Moratalla R, Graybiel AM, White FJ, Tonegawa S (1994) Elimination of cocaine-induced hyperactivity and dopamine-mediated neurophysiological effects in dopamine D1 receptor mutant mice. Cell 79:945–955.

Yano H, Cai NS, Xu M, Verma RK, Rea W, Hoffman AF, Shi L, Javitch JA, Bonci A, Ferré S (2018) Gs- versus Golf-dependent functional selectivity mediated by the dopamine D1 receptor. Nat Commun 9:486.

Yim YY, Betke KM, McDonald WH, Gilsbach R, Chen Y, Hyde K, Wang Q, Hein L, Hamm HE (2020) Author correction: the in vivo specificity of synaptic Gbeta and Ggamma subunits to the alpha2a adrenergic receptor at CNS synapses. Sci Rep 10:2966.

Zhuang X, Belluscio L, Hen R (2000) G(olf)alpha mediates dopamine D1 receptor signaling. J Neurosci 20:RC91.